

# SPECIALIZATION PROJECT IN THEORETICAL PHYSICS

---

## Supercurrent transport by Andreev Bound States in external field

---

*Author:*

Anna Ursula Birkeland BRØYN

*Supervisor*

Prof. Jacob Linder

December 14, 2016



**NTNU – Trondheim**  
Norwegian University of  
Science and Technology

## Abstract

Here you give a summary of your work and your results. This is like a management summary and should be written in a clear and easy language, without many difficult terms and without abbreviations. Everything you present here must be treated in more detail in the main report. You should not give any references to the report in the summary – just explain what you have done and what you have found out. The Summary and Conclusions should be no more than two pages.

You may assume that you have got three minutes to present to the Rector of NTNU what you have done and what you have found out as part of your thesis. (He is an intelligent person, but does not know much about your field of expertise.)

## Acknowledgement

I would like to thank the following persons for their great help during ...

If the project has been carried out in cooperation with an external partner (e.g., a company), you should acknowledge the contribution and give thanks to the involved persons.

You should also acknowledge the contributions made by your supervisor(s).

O.N.

(Your initials)

# Contents

<b>Abstract</b>	<b>i</b>
<b>Acknowledgement</b>	<b>ii</b>
<b>Contents</b>	<b>iii</b>
<b>Abbreviations</b>	<b>v</b>
<b>1 Introduction</b>	<b>1</b>
<b>2 Superconductivity</b>	<b>2</b>
2.1 The Meissner effect . . . . .	2
2.2 BCS theory . . . . .	3
2.2.1 The BCS Hamiltonian . . . . .	3
2.2.2 Mean field Approximation . . . . .	4
2.2.3 Diagonalization of the BCS Hamiltonian . . . . .	6
2.2.4 Bogoliubov-de Gennes Equations . . . . .	8
2.3 Andreev reflection . . . . .	9
2.4 Josephson current . . . . .	11
2.5 Free Energy . . . . .	12
<b>3 Physical System</b>	<b>14</b>
<b>4 Andreev Bound State energies in SNS-junction</b>	<b>17</b>
4.1 ABS energies without barriers or applied field . . . . .	17
4.1.1 Andreev reflection amplitude . . . . .	18

4.1.2 Bohr-Sommerfeld quantization . . . . .	19
4.1.3 ABS energy . . . . .	20
4.2 ABS energies with barriers . . . . .	20
4.2.1 Boundary conditions . . . . .	20
4.2.2 Wave functions in the superconduction region . . . . .	21
4.2.3 Wave functions in the normal region . . . . .	24
4.2.4 ABS energy . . . . .	24
4.3 ABS energies with applied field . . . . .	26
4.3.1 Guage transformation . . . . .	26
4.3.2 Bohr-Sommerfeld quantization condition . . . . .	27
4.3.3 ABS energy . . . . .	28
<b>5 Andreev Bound State Current in SNS-junction</b>	<b>29</b>
5.1 ABS current without barriers or applied field . . . . .	30
5.2 ABS current with barriers . . . . .	31
5.3 ABS current with applied field . . . . .	32
5.3.1 Uniform magnetic field . . . . .	32
5.3.2 Sinusoidal field varying along the junction . . . . .	35
5.3.3 Sinusoidal field varying along the interfaces . . . . .	40
<b>6 Conclusion and outlook</b>	<b>45</b>
<b>A Additional Information</b>	<b>47</b>
A.1 Commutation relations . . . . .	47
A.2 The pauli matrices . . . . .	47
<b>Bibliography</b>	<b>48</b>

# **Abbreviations**

**FTA** Fault tree analysis

**MTTF** Mean time to failure

**RAMS** Reliability, availability, maintainability, and safety

# **Chapter 1**

## **Introduction**

# Chapter 2

## Superconductivity

Two fundamental properties associated to superconductivity are 1) zero electrical resistance giving rise to *supercurrents*, for temperatures below some critical temperature  $T_c$  and 2) complete expulsion of magnetic field below  $T_c$ , known as the Meissner effect [1, 2]. The theory behind these properties was presented by Bardeen, Cooper and Schrieffer in 1957 and is known as the BCS-theory [3].

### 2.1 The Meissner effect

Meissner and Ochsenfeld discovered in 1933 [1] that applied magnetic field,  $H$ , below some critical limit  $H_c$ , would be expelled in the superconductor for temperatures below  $T_c$ , resulting in zero field inside the superconductor,  $B = \mu_0(H+M) = 0$ , so that  $M = -H$ . The superconductor is thus a perfect diamagnet with susceptibility

$$\chi = \frac{dM}{dH} = -1. \quad (2.1)$$

This is called the Meissner effect and is a consequence of induced screening supercurrents at the surface of the superconductor. No current can exist only on the surface of a material as this would imply a finite current in a layer of zero thickness requiring infinite density of free charge. Consequently, the screening current must exist at some finite distance,  $\lambda_L$ , into the superconductor and thus letting the external magnetic field penetrate to a depth  $\lambda_L$ . This penetration

depth will depend on the density of superconducting carriers (Cooper pairs) and is a result from the London equations [4] and Ampere's law.

The Meissner effect breaks down as the external field is increased to above the critical limit  $H_c$ . Depending on the material we will then get full (in type I superconductors) or partial (in type II superconductors) penetration of magnetic flux and the superconductor will go from the superconducting state into the normal or mixed state, respectively.

## 2.2 BCS theory

The BCS theory is based on the appearance of so called *Cooper pairs* which conventionally are formed by a phonon-mediated attractive interaction between two electrons overwinning the Coulomb repulsion [3]. The Cooper pairs are bosonic...

### 2.2.1 The BCS Hamiltonian

The Hamiltonian of the system will consist of two parts, describing the non-interacting and interacting electrons, respectively. A given state is defined by the momentum  $\mathbf{k}$  and spin  $\sigma$ . In the second quantization formalism the annihilation- and creation operators,  $c_{\mathbf{k},\sigma}$  and  $c_{\mathbf{k},\sigma}^\dagger$ , will destroy and create an electron in the corresponding state, respectively. The number operator  $n_{\mathbf{k},\sigma} = c_{\mathbf{k},\sigma}^\dagger c_{\mathbf{k},\sigma}$  counts the number of electrons in the state. The non-interacting part of the Hamiltonian will simply be the energy of each state,  $\epsilon_{\mathbf{k}} = \hbar^2 k^2 / 2m$ , times the number operator and summed over all states. This will thus be the first term in Hamiltonian (2.2). The interacting part of the Hamiltonian will describe a scattering process where two electrons into the states  $(\mathbf{k}, \sigma)$  and  $(\mathbf{k}', \sigma')$  are scattered to the states  $(\mathbf{k} + \mathbf{q}, \sigma)$  and  $(\mathbf{k}' - \mathbf{q}, \sigma')$ , i.e.  $(\mathbf{k}, \sigma)$  and  $(\mathbf{k} + \mathbf{q}, \sigma)$  are destroyed by the annihilation operators while  $(\mathbf{k}' - \mathbf{q}, \sigma')$  and  $(\mathbf{k}', \sigma')$  are created by the creation operators. We must also include a matrix element  $V_{\mathbf{k},\mathbf{k}'}$  including both the attractive phonon-mediated interaction and the repulsive Coulomb interaction, between the electrons. The second term in the Hamiltonian (2.2) describe this interaction. The total Hamiltonian in-

cluding both the non-interacting and the interacting term is thus given as

$$H = \sum_{\mathbf{k}, \sigma} \epsilon_{\mathbf{k}} c_{\mathbf{k}, \sigma}^\dagger c_{\mathbf{k}, \sigma} + \sum_{\mathbf{k}, \mathbf{k}', \mathbf{q}, \sigma, \sigma'} V_{\mathbf{k}, \mathbf{k}'}(\mathbf{q}, \omega) c_{\mathbf{k}+\mathbf{q}, \sigma}^\dagger c_{\mathbf{k}'-\mathbf{q}, \sigma'}^\dagger c_{\mathbf{k}, \sigma} c_{\mathbf{k}', \sigma'}. \quad (2.2)$$

We define  $\epsilon_{\mathbf{k}} \equiv \epsilon_{\mathbf{k}} - \mu$  as the energy above the Fermi surface. We have used the chemical potential,  $\mu$ , in the place of the Fermi energy,  $\epsilon_F$ , as these two quantities are essentially the same in all relevant cases. The attractive interaction will only be valid in a small energy range,  $\omega$ , above the Fermi-surface, and for electrons on opposite sides of the Fermi-surface. We may therefore let  $\mathbf{k}' = -\mathbf{k}$ . Due to the Pauli principle we will in most cases find the electrons in the Cooper pairs in opposite spin states, so we will also let  $\sigma' = -\sigma$ . By now changing the dummy indices, the Hamiltonian takes the form

$$H - \mu N = \sum_{\mathbf{k}, \sigma} \epsilon_{\mathbf{k}} c_{\mathbf{k}, \sigma}^\dagger c_{\mathbf{k}, \sigma} + \sum_{\mathbf{k}, \mathbf{k}'} V_{\mathbf{k}, \mathbf{k}'} c_{\mathbf{k}, \uparrow}^\dagger c_{-\mathbf{k}, \downarrow}^\dagger c_{\mathbf{k}', \uparrow} c_{-\mathbf{k}', \downarrow}, \quad (2.3)$$

where  $N$  is the number of electrons. Henceforth we will write  $H$  in place of  $H - \mu N$ .

### 2.2.2 Mean field Approximation

We will use mean field approximation to simplify the Hamiltonian and assume the fluctuations around the expectation values to be small such that we can write

$$c_{-\mathbf{k}, \downarrow} c_{\mathbf{k}, \uparrow} = \langle c_{-\mathbf{k}, \downarrow} c_{\mathbf{k}, \uparrow} \rangle + c_{-\mathbf{k}, \downarrow} c_{\mathbf{k}, \uparrow} - \langle c_{-\mathbf{k}, \downarrow} c_{\mathbf{k}, \uparrow} \rangle \equiv \langle c_{-\mathbf{k}, \downarrow} c_{\mathbf{k}, \uparrow} \rangle + \delta_{\mathbf{k}}, \quad (2.4)$$

and only keep  $\delta$  to the first order. By also defining the *gap parameter* as follows

$$\Delta_{\mathbf{k}'} = \sum_{\mathbf{k}} V_{\mathbf{k}, \mathbf{k}'} \langle c_{-\mathbf{k}, \downarrow} c_{\mathbf{k}, \uparrow} \rangle, \quad (2.5)$$

the Hamiltonian will simplify to

$$\begin{aligned}
H &= \sum_{\mathbf{k},\sigma} \varepsilon_{\mathbf{k}} c_{\mathbf{k},\sigma}^\dagger c_{\mathbf{k},\sigma} + \sum_{\mathbf{k}} \left[ \Delta_{\mathbf{k}}^* c_{\mathbf{k},\uparrow} c_{-\mathbf{k},\downarrow} + \Delta_{\mathbf{k}} c_{\mathbf{k},\uparrow}^\dagger c_{-\mathbf{k},\downarrow}^\dagger - \Delta_{\mathbf{k}} \langle c_{\mathbf{k},\uparrow}^\dagger c_{-\mathbf{k},\downarrow} \rangle \right] \\
&= - \sum_{\mathbf{k}} \Delta_{\mathbf{k}} \langle c_{\mathbf{k},\uparrow}^\dagger c_{-\mathbf{k},\downarrow} \rangle + \sum_{\mathbf{k}} \varepsilon_{\mathbf{k}} \left[ c_{\mathbf{k},\uparrow}^\dagger c_{\mathbf{k},\uparrow} + c_{-\mathbf{k},\downarrow}^\dagger c_{-\mathbf{k},\downarrow} \right] + \sum_{\mathbf{k}} \left[ \Delta_{\mathbf{k}}^* c_{\mathbf{k},\uparrow} c_{-\mathbf{k},\downarrow} + \Delta_{\mathbf{k}} c_{\mathbf{k},\uparrow}^\dagger c_{-\mathbf{k},\downarrow}^\dagger \right] \\
&= \sum_{\mathbf{k}} \left[ \varepsilon_{\mathbf{k}} - \Delta_{\mathbf{k}} \langle c_{\mathbf{k},\uparrow}^\dagger c_{-\mathbf{k},\downarrow} \rangle \right] + \sum_{\mathbf{k}} \varepsilon_{\mathbf{k}} \left[ c_{\mathbf{k},\uparrow}^\dagger c_{\mathbf{k},\uparrow} - c_{-\mathbf{k},\downarrow} c_{-\mathbf{k},\downarrow}^\dagger \right] + \sum_{\mathbf{k}} \left[ \Delta_{\mathbf{k}}^* c_{\mathbf{k},\uparrow} c_{-\mathbf{k},\downarrow} + \Delta_{\mathbf{k}} c_{\mathbf{k},\uparrow}^\dagger c_{-\mathbf{k},\downarrow}^\dagger \right] \quad (2.6) \\
&= E_0 + \sum_{\mathbf{k}} \begin{pmatrix} c_{\mathbf{k},\uparrow}^\dagger & c_{-\mathbf{k},\downarrow} \end{pmatrix} \begin{pmatrix} \varepsilon_{\mathbf{k}} & \Delta_{\mathbf{k}} \\ \Delta_{\mathbf{k}}^* & -\varepsilon_{\mathbf{k}} \end{pmatrix} \begin{pmatrix} c_{\mathbf{k},\uparrow} \\ c_{-\mathbf{k},\downarrow}^\dagger \end{pmatrix} \equiv E_0 + \sum_{\mathbf{k}} \varphi_{\mathbf{k}}^\dagger H'_{\mathbf{k}} \varphi_{\mathbf{k}}
\end{aligned}$$

where we have used the standard commutation relations for fermions (A.1c) and defined

$$E_0 \equiv \sum_{\mathbf{k}} \left[ \varepsilon_{\mathbf{k}} - \Delta_{\mathbf{k}} \langle c_{\mathbf{k},\uparrow}^\dagger c_{-\mathbf{k},\downarrow} \rangle \right], \quad H'_{\mathbf{k}} = \begin{pmatrix} \varepsilon_{\mathbf{k}} & \Delta_{\mathbf{k}} \\ \Delta_{\mathbf{k}}^* & -\varepsilon_{\mathbf{k}} \end{pmatrix} \quad \text{and} \quad \varphi'_{\mathbf{k}} \equiv \begin{pmatrix} c_{\mathbf{k},\uparrow} \\ c_{-\mathbf{k},\downarrow}^\dagger \end{pmatrix}.$$

The Hamiltonian (2.6) can be diagonalized by inserting  $U_{\mathbf{k}} U_{\mathbf{k}}^\dagger = I$ , where  $U$  is a unitary matrix:

$$U_{\mathbf{k}} = \begin{pmatrix} u_{\mathbf{k}} & -v_{\mathbf{k}}^* \\ v_{\mathbf{k}} & u_{\mathbf{k}}^* \end{pmatrix}, \quad U_{\mathbf{k}}^\dagger = \begin{pmatrix} u_{\mathbf{k}}^* & v_{\mathbf{k}}^* \\ -v_{\mathbf{k}} & u_{\mathbf{k}} \end{pmatrix} \quad (2.7)$$

and  $u_{\mathbf{k}}$  and  $v_{\mathbf{k}}$  satisfy the relation

$$|u_{\mathbf{k}}|^2 + |v_{\mathbf{k}}|^2 = 1. \quad (2.8)$$

This will be satisfied if we write  $u_{\mathbf{k}}$  and  $v_{\mathbf{k}}$  on the form

$$u_{\mathbf{k}} = e^{i\alpha} \cos \theta_{\mathbf{k}}, \quad v_{\mathbf{k}} = e^{i\beta} \sin \theta_{\mathbf{k}}. \quad (2.9)$$

Our Hamiltonian will now be on the form

$$H = E_0 + \sum_{\mathbf{k}} \varphi_{\mathbf{k}}^\dagger H_{\mathbf{k}} \varphi_{\mathbf{k}} \quad (2.10)$$

with  $H_{\mathbf{k}} = U_{\mathbf{k}}^\dagger H'_{\mathbf{k}} U_{\mathbf{k}}$  and  $\varphi_{\mathbf{k}} \equiv U_{\mathbf{k}}^\dagger \varphi'_{\mathbf{k}}$ , i.e.

$$\varphi_{\mathbf{k}} \equiv \begin{pmatrix} \gamma_{\mathbf{k},\uparrow} \\ \gamma_{-\mathbf{k},\downarrow}^\dagger \end{pmatrix} = \begin{pmatrix} u_{\mathbf{k}}^* & v_{\mathbf{k}}^* \\ -v_{\mathbf{k}} & u_{\mathbf{k}} \end{pmatrix} \begin{pmatrix} c_{\mathbf{k},\uparrow} \\ c_{-\mathbf{k},\downarrow}^\dagger \end{pmatrix}. \quad (2.11)$$

The new fermionic operators  $\gamma_{\mathbf{k},\uparrow}$  and  $\gamma_{-\mathbf{k},\downarrow}^\dagger$  are describing excitations of so called *quasiparticles*.

### 2.2.3 Diagonalization of the BCS Hamiltonian

We need to find what values of  $u_{\mathbf{k}}$  and  $v_{\mathbf{k}}$  that will satisfy the relation (2.8) and diagonalize  $H_{\mathbf{k}}$ :

$$\begin{aligned} H_{\mathbf{k}} &= U_{\mathbf{k}}^\dagger H'_{\mathbf{k}} U_{\mathbf{k}} = \begin{pmatrix} u_{\mathbf{k}}^* & v_{\mathbf{k}}^* \\ -v_{\mathbf{k}} & u_{\mathbf{k}} \end{pmatrix} \begin{pmatrix} \varepsilon_{\mathbf{k}} & \Delta_{\mathbf{k}} \\ \Delta_{\mathbf{k}}^* & -\varepsilon_{\mathbf{k}} \end{pmatrix} \begin{pmatrix} u_{\mathbf{k}} & -v_{\mathbf{k}}^* \\ v_{\mathbf{k}} & u_{\mathbf{k}}^* \end{pmatrix} \\ &= \begin{pmatrix} \varepsilon_{\mathbf{k}}(|u_{\mathbf{k}}|^2 - |v_{\mathbf{k}}|^2) + \Delta_{\mathbf{k}} u_{\mathbf{k}}^* v_{\mathbf{k}} + \Delta_{\mathbf{k}}^* u_{\mathbf{k}} v_{\mathbf{k}}^* & \Delta_{\mathbf{k}} u_{\mathbf{k}}^{*2} - \Delta_{\mathbf{k}}^* v_{\mathbf{k}}^{*2} - 2\varepsilon_{\mathbf{k}} u_{\mathbf{k}}^* v_{\mathbf{k}}^* \\ \Delta_{\mathbf{k}}^* u_{\mathbf{k}}^2 - \Delta_{\mathbf{k}} v_{\mathbf{k}}^2 - 2\varepsilon_{\mathbf{k}} u_{\mathbf{k}} v_{\mathbf{k}} & -[\varepsilon_{\mathbf{k}}(|u_{\mathbf{k}}|^2 - |v_{\mathbf{k}}|^2) + \Delta_{\mathbf{k}} u_{\mathbf{k}}^* v_{\mathbf{k}} + \Delta_{\mathbf{k}}^* u_{\mathbf{k}} v_{\mathbf{k}}^*] \end{pmatrix}. \end{aligned} \quad (2.12)$$

For the off-diagonal elements to be zero we must have  $\Delta_{\mathbf{k}}^* u_{\mathbf{k}}^2 - \Delta_{\mathbf{k}} v_{\mathbf{k}}^2 - 2\varepsilon_{\mathbf{k}} u_{\mathbf{k}} v_{\mathbf{k}} = 0$ . We write  $u_{\mathbf{k}}$  and  $v_{\mathbf{k}}$  on the form given in equation (2.9) and write  $\Delta_{\mathbf{k}} = |\Delta_{\mathbf{k}}| e^{i\varphi}$ . This yields

$$\begin{aligned} 0 &= \Delta_{\mathbf{k}}^* u_{\mathbf{k}}^2 - \Delta_{\mathbf{k}} v_{\mathbf{k}}^2 - 2\varepsilon_{\mathbf{k}} u_{\mathbf{k}} v_{\mathbf{k}} \\ &= |\Delta_{\mathbf{k}}| e^{i(\alpha+\beta)} \cos^2 \theta \left( e^{i(\alpha-\beta-\varphi)} - e^{-i(\alpha-\beta-\varphi)} \tan^2 \theta_{\mathbf{k}} - 2 \frac{\varepsilon_{\mathbf{k}}}{|\Delta_{\mathbf{k}}|} \tan \theta_{\mathbf{k}} \right), \end{aligned}$$

which gives

$$\alpha - \beta = \varphi \quad \text{and} \quad \tan \theta_{\mathbf{k}} = -\frac{\varepsilon_{\mathbf{k}}}{|\Delta_{\mathbf{k}}|} \pm \sqrt{\frac{\varepsilon_{\mathbf{k}}^2}{|\Delta_{\mathbf{k}}|^2} + 1}. \quad (2.13)$$

$u_{\mathbf{k}}$  and  $v_{\mathbf{k}}$  will thus be satisfied by

$$\begin{aligned} |u_{\mathbf{k}}|^2 &= \cos^2 \theta = \frac{1}{2} \left( 1 \pm \frac{\varepsilon_{\mathbf{k}}^\pm}{\sqrt{\varepsilon_{\mathbf{k}}^{\pm 2} + |\Delta_{\mathbf{k}}|^2}} \right) \\ |v_{\mathbf{k}}|^2 &= \sin^2 \theta = \frac{1}{2} \left( 1 \mp \frac{\varepsilon_{\mathbf{k}}^\pm}{\sqrt{\varepsilon_{\mathbf{k}}^{\pm 2} + |\Delta_{\mathbf{k}}|^2}} \right). \end{aligned} \quad (2.14)$$

We let  $\varepsilon_{\mathbf{k}}^+ > 0$  and  $\varepsilon_{\mathbf{k}}^- < 0$  and notice that we get  $|u_{\mathbf{k}}| = 1$  and  $|v_{\mathbf{k}}| = 0$  when  $\Delta_{\mathbf{k}} = 0$ , i.e. when there is no attraction between the electrons and thus in the limit of the *normal* state, according to equation (2.5). We calculate the diagonal terms of  $H_{\mathbf{k}}$  (2.12) and find

$$H_{\mathbf{k}} = \begin{pmatrix} E_{\mathbf{k}} & 0 \\ 0 & -E_{\mathbf{k}} \end{pmatrix} \quad (2.15)$$

where we have defined

$$E_{\mathbf{k}} = \sqrt{\varepsilon_{\mathbf{k}}^2 + |\Delta_{\mathbf{k}}|^2}. \quad (2.16)$$

as the quasiparticle excitation energy. It is now clear why  $\Delta_{\mathbf{k}}$  is referred to as the *gap-parameter* as it gives a gap in the excitation spectrum of the quasiparticles  $\varphi_{\mathbf{k}}$ . Moreover, we get

$$k^{\pm} = k_F \sqrt{1 + \frac{\varepsilon_{\mathbf{k}}^{\pm}}{\mu}} = k_F \sqrt{1 \pm \frac{\sqrt{E_{\mathbf{k}}^2 - |\Delta_{\mathbf{k}}|^2}}{\mu}} \quad (2.17)$$

where  $\mu = \hbar^2 k_F / 2m$  and  $\varepsilon_{\mathbf{k}}^{\pm} = \pm \sqrt{E_{\mathbf{k}} - |\Delta_{\mathbf{k}}|^2}$  is obtained from equation (2.16). We notice how we get a fourfold degeneracy of relevant states,  $(k^+, k^-, -k^+, -k^-)$ , for each  $E_{\mathbf{k}}$ . From equation (2.14) we see that the quasiparticle excitation  $\gamma_{\mathbf{k},\uparrow}^\dagger$  from equation (2.11) will be electronlike, since we have  $u_{\mathbf{k}} \rightarrow 1$  and  $v_{\mathbf{k}} \rightarrow 0$  as  $\Delta \rightarrow 0$  and  $c_{\mathbf{k},\uparrow}^\dagger$  creates an electron while  $c_{-\mathbf{k},\downarrow}$  destroys an electron, leaving a hole. Similarly,  $\gamma_{\mathbf{k},\uparrow}$  will be hololike. Moreover, from equation (2.17) we see that  $\pm k^+$  ( $\pm k^-$ ) corresponds to energy above(below) the Fermi surface and thus  $\pm k^+$  ( $\pm k^-$ ) are electron(hole)-like excitations.

For convenience we introduce a new variable,  $\eta$ , defined in the following way

$$\eta = \begin{cases} \arccos\left(\frac{E_{\mathbf{k}}}{|\Delta_{\mathbf{k}}|}\right), & \text{if } E_{\mathbf{k}} < |\Delta_{\mathbf{k}}| \\ i \operatorname{arccosh}\left(\frac{E_{\mathbf{k}}}{|\Delta_{\mathbf{k}}|}\right), & \text{if } E_{\mathbf{k}} > |\Delta_{\mathbf{k}}|. \end{cases} \quad (2.18)$$

Then we can write

$$\frac{|u_{\mathbf{k}}|}{|v_{\mathbf{k}}|} = e^{i\eta}. \quad (2.19)$$

### 2.2.4 Bogoliubov-de Gennes Equations

In the description above we assumed the Hamiltonian to be position-invariant so that the wave functions could be considered as simple plane waves,  $\sim \exp(i\mathbf{k} \cdot \mathbf{r})$ . We took the potential  $V(\mathbf{r})$  and the vector potential,  $\mathbf{A}$ , to be zero and the simply replaced the Hamiltonian for a single particle system,

$$h(\mathbf{r}) = \frac{1}{2m} \left( \frac{\hbar}{i} \nabla - q\mathbf{A} \right)^2 - \mu(\mathbf{r}) + V(\mathbf{r}), \quad (2.20)$$

with  $\varepsilon_{\mathbf{k}} = \hbar^2 k^2 / 2m - \mu$ . For systems where we can not do this simplification we introduce field operators:

$$\psi(\mathbf{r}, t) \equiv \sum_{\mathbf{k}} U(\mathbf{r}, t) \varphi_{\mathbf{k}}, \quad \psi^\dagger(\mathbf{r}, t) \equiv \sum_{\mathbf{k}} \varphi_{\mathbf{k}}^\dagger U^\dagger(\mathbf{r}, t) \quad (2.21)$$

and rewrite the Hamiltonian in equation (2.6) as

$$H = E_0 + \int d^3 r \psi^\dagger(\mathbf{r}, t) \begin{pmatrix} h(\mathbf{r}) & \Delta(\mathbf{r}) \\ \Delta^*(\mathbf{r}) & -h(\mathbf{r}) \end{pmatrix} \psi(\mathbf{r}, t) \equiv E_0 + \int d^3 r \psi^\dagger(\mathbf{r}, t) H(\mathbf{r}) \psi(\mathbf{r}, t). \quad (2.22)$$

Again the Hamiltonian may be diagonalized by setting  $U^\dagger(\mathbf{r}, t) H(\mathbf{r}) U(\mathbf{r}, t) = H_{\mathbf{k}}$ , or equally  $H(\mathbf{r}) U(\mathbf{r}, t) = U(\mathbf{r}, t) H_{\mathbf{k}}$ , where  $H_{\mathbf{k}}$  is on the form given in equation (2.15). By separating these equations for each eigenvalue in  $H_{\mathbf{k}}$  we get the *Bogoliubov de Gennes equations* (BdG equations) [5]:

$$\begin{aligned} \begin{pmatrix} h(\mathbf{r}) & \Delta(\mathbf{r}) \\ \Delta^*(\mathbf{r}) & -h(\mathbf{r}) \end{pmatrix} \begin{pmatrix} u(\mathbf{r}, t) \\ v(\mathbf{r}, t) \end{pmatrix} &= E_{\mathbf{k}} \begin{pmatrix} u(\mathbf{r}, t) \\ v(\mathbf{r}, t) \end{pmatrix}, \\ \begin{pmatrix} -h(\mathbf{r}) & -\Delta^*(\mathbf{r}) \\ -\Delta(\mathbf{r}) & h(\mathbf{r}) \end{pmatrix} \begin{pmatrix} -v(\mathbf{r}, t) \\ u(\mathbf{r}, t) \end{pmatrix} &= E_{\mathbf{k}} \begin{pmatrix} -v(\mathbf{r}, t) \\ u(\mathbf{r}, t) \end{pmatrix}. \end{aligned} \quad (2.23)$$

From equation (2.11) we have  $\gamma_{\mathbf{k},\uparrow}^\dagger = u(\mathbf{r}, t) c_{\mathbf{k},\uparrow}^\dagger + v(\mathbf{r}, t) c_{-\mathbf{k},\downarrow}$ . By writing  $\gamma_{\mathbf{k},\sigma}^\dagger = u_\sigma(\mathbf{r}, t) c_{\mathbf{k},\sigma}^\dagger + v_{-\sigma}(\mathbf{r}, t) c_{-\mathbf{k},-\sigma}$  and  $\gamma_{\mathbf{k},\sigma} = u_\sigma(\mathbf{r}, t) c_{-\mathbf{k},-\sigma}^\dagger + v_{-\sigma}(\mathbf{r}, t) c_{\mathbf{k},\sigma}$ , we can represent  $\gamma_{\mathbf{k},\sigma}^\dagger$  and  $\gamma_{\mathbf{k},\sigma}$  by the vectors  $\Psi_{e,\sigma}$  and

$\Psi_{h,\sigma}$ , respectively, where  $\Psi$  is a vector of the form  $(u_\uparrow, u_\downarrow, v_\uparrow, v_\downarrow)^T$ . We get:

$$\begin{aligned} \gamma_{\mathbf{k},\uparrow}^\dagger \rightarrow \Psi_{e,\uparrow} &= \begin{pmatrix} u(\mathbf{r}, t) \\ 0 \\ 0 \\ v(\mathbf{r}, t) \end{pmatrix}, & \gamma_{-\mathbf{k},\downarrow}^\dagger \rightarrow \Psi_{e,\downarrow} &= \begin{pmatrix} 0 \\ u(\mathbf{r}, t) \\ -v(\mathbf{r}, t) \\ 0 \end{pmatrix}, \\ \gamma_{\mathbf{k},\uparrow} \rightarrow \Psi_{h,\uparrow} &= \begin{pmatrix} v^*(\mathbf{r}, t) \\ 0 \\ 0 \\ u^*(\mathbf{r}, t) \end{pmatrix}, & \gamma_{-\mathbf{k},\downarrow} \rightarrow \Psi_{h,\downarrow} &= \begin{pmatrix} 0 \\ -v^*(\mathbf{r}, t) \\ u^*(\mathbf{r}, t) \\ 0 \end{pmatrix}. \end{aligned} \quad (2.24)$$

We define the  $2 \times 2$ -matrices  $\hat{H}(\mathbf{r}) \equiv \hat{\sigma}_0 h(\mathbf{r})$  and  $\hat{\Delta}(\mathbf{r}) \equiv i\hat{\sigma}_2 \Delta(\mathbf{r})$  where  $\hat{\sigma}_0$  is the identity matrix and  $\hat{\sigma}_i$  with  $(i = 1, 2, 3)$  are the Pauli matrices, see equation (A.2) in the appendix. Moreover, we define  $\vec{u}(\mathbf{r}, t) \equiv (u_\uparrow(\mathbf{r}, t) \ u_\downarrow(\mathbf{r}, t))^T$  and  $\vec{v}(\mathbf{r}, t) \equiv (v_\uparrow(\mathbf{r}, t) \ v_\downarrow(\mathbf{r}, t))^T$ . The BdG-equations (2.23) can then be written more compact:

$$\begin{pmatrix} \hat{H}(\mathbf{r}) & \hat{\Delta}(\mathbf{r}) \\ \hat{\Delta}^\dagger(\mathbf{r}) & -\hat{H}(\mathbf{r}) \end{pmatrix} \begin{pmatrix} \vec{u}(\mathbf{r}, t) \\ \vec{v}(\mathbf{r}, t) \end{pmatrix} = E_{\mathbf{k}} \begin{pmatrix} \vec{u}(\mathbf{r}, t) \\ \vec{v}(\mathbf{r}, t) \end{pmatrix}. \quad (2.25)$$

## 2.3 Andreev reflection

When an electron with momentum,  $\mathbf{k}^+ = k_x^+ \hat{x} + k_y^+ \hat{y} + k_z^+ \hat{z}$ , and spin,  $\sigma$ , in the normal metal is propagating towards the interface between the normal metal and a superconductor, it will be scattered with certain probabilities of transmission and reflection. We choose the coordinate system such that the intersection is placed in the  $yz$ -plane, see figure !!!REFFIG!!!. There are two possible ways the electron could be transmitted and reflected. The electron may be transmitted into the superconductor as an electron-like quasiparticle such that the energy of the transmitted quasiparticle is on the *same* side of the Fermi surface, i.e. with momentum  $\mathbf{q}^+ = q_x^+ \hat{x} + q_y^+ \hat{y} + q_z^+ \hat{z}$  and spin  $\sigma$ , or as a hole-like quasiparticle by crossing the Fermi surface, i.e. with momentum  $\mathbf{q}^- = -q_x^- \hat{x} + q_y^- \hat{y} + q_z^- \hat{z}$  and spin  $\sigma$ . The  $x$ -component have negative sign since the wave direction of a hole is opposite of the direction of its wave vector, as explained in section 2.2.3 !!!OBS

PASS PÅ AT DETTE ER FORKLART RETT STED!!!. The electron may be reflected, either in the normal way, i.e. as an electron with momentum,  $\mathbf{k}_r^+ = -k_x^+ \hat{x} + k_y^+ \hat{y} + k_z^+ \hat{z}$ , and the same spin,  $\sigma$ , or by *Andreev reflection* [6]. In Andreev reflection the incoming electron goes into the superconductor and form a Cooper pair with an electron of opposite spin, leaving a reflected hole with momentum  $\mathbf{k}^- = k_x^- \hat{x} + k_y^- \hat{y} + k_z^- \hat{z}$  and spin  $-\sigma$ . We will in this section ignore the spin degeneracy and express the wave vectors as  $\psi(\mathbf{r}) = (u_{\mathbf{k}}(\mathbf{r}) \ v_{\mathbf{k}}(\mathbf{r}))^T$ . In the simplest case we consider plane waves, i.e. energies,  $E_{\mathbf{k}}$ , as given in equation (2.16) with corresponding wave numbers,  $\mathbf{k}^\pm$  and wave vectors of the form [7]

$$\psi_{k^+}(\mathbf{r}) = \begin{pmatrix} u_0 e^{i\alpha} \\ v_0 e^{i\beta} \end{pmatrix} e^{i\mathbf{k}^+ \cdot \mathbf{r}} \quad \text{and} \quad \psi_{k^-}(\mathbf{r}) = \begin{pmatrix} v_0 e^{-i\beta} \\ u_0 e^{-i\alpha} \end{pmatrix} e^{i\mathbf{k}^- \cdot \mathbf{r}}, \quad (2.26)$$

in correspondance with equation (2.24). The incoming, reflected and transmitted wave vectors will in this notation take the form

$$\begin{aligned} \psi_i(\mathbf{r}) &= \begin{pmatrix} 1 \\ 0 \end{pmatrix} e^{i\mathbf{k}^+ \cdot \mathbf{r}} \\ \psi_r(\mathbf{r}) &= r_{ee} \begin{pmatrix} 1 \\ 0 \end{pmatrix} e^{i\mathbf{k}_r^+ \cdot \mathbf{r}} + r_{eh} \begin{pmatrix} 0 \\ 1 \end{pmatrix} e^{i\mathbf{k}^- \cdot \mathbf{r}} \\ \psi_t(\mathbf{r}) &= t_{ee} \begin{pmatrix} u_0 e^{i\alpha} \\ v_0 e^{i\beta} \end{pmatrix} e^{i\mathbf{q}^+ \cdot \mathbf{r}} + t_{eh} \begin{pmatrix} v_0 e^{-i\beta} \\ u_0 e^{-i\alpha} \end{pmatrix} e^{i\mathbf{q}^- \cdot \mathbf{r}}, \end{aligned} \quad (2.27)$$

where  $r_{ee}$ ,  $r_{eh}$ ,  $t_{ee}$ , and  $t_{eh}$  represent the probabilities of normal reflection, Andreev reflection, electron-like transmission and hole-like transmission, respectively. We notice how the normal reflection will give opposite value of the  $x$ -component of the wave vector while the others remain the same. In the Andreev reflection, however, we have retro reflection and the hole will thus move along the same path as the incoming electron. See figure !!!!FIGREF!!!!.

In equation (2.16) we found that only energies above the energy gap,  $|\Delta_{\mathbf{k}}|$ , are allowed for the quasiparticles. Consequently, when  $E_{\mathbf{k}} < |\Delta_{\mathbf{k}}|$  the amplitudes  $t_{ee}$  and  $t_{eh}$  will be zero and only reflection (either normal or Andreev reflection) is allowed. If there is no barrier at the interface,

there will be no normal reflection and only Andreev reflection will be allowed. States with such energies in SNS-junctions would thus be trapped in the normal metal by the Andreev reflections and are referred to as Andreev Bound States (ABS).

## 2.4 Josephson current

A Josephson junction is a device consisting of two superconductors that is brought into contact via a *weak link*, in which the *critical current* is much lower. The critical current is the maximum supercurrent that can exist in the superconductor and is related to the density of Cooper pairs. Josephson effect describes two important phenomena of supercurrents in a Josephson junction [8]. Firstly Josephson predicted that supercurrents would flow through the Josephson junction even without any applied voltage. Secondly if the junction was driven by an external current exceeding the critical current, electromagnetic waves would be radiated. We will here focus on the first phenomena.

There are several ways to construct a weak link, and we will in this project consider the *SNS-junction*, i.e. a junction consisting of two superconductors, separated by a normal metal.

The Josephson current is in general dependent on the full quasiparticle spectrum, but in the short junction regime the continuous spectrum ( $E > \Delta_0$ ) does not contribute to the current.  
blblbabla

The number operator,  $N$ , of the Cooper pairs in the superconductor, and the superconducting phase  $\varphi$  are canonical conjugate variables. Hence

$$\dot{N} = -\frac{1}{\hbar} \frac{\partial H}{\partial \varphi} \quad \dot{\varphi} = \frac{1}{\hbar} \frac{\partial H}{\partial N}. \quad (2.28)$$

The tunnelig current from a superconductor  $S_1$  with number of particles  $N_1$  to a superconductor  $S_2$  with number of particles  $N_2$  through a weak link will be given as

$$I = q \dot{N}_1 = -q \dot{N}_2 \quad (2.29)$$

where  $q = -2e$  is the charge of a Cooper pair. Using equation (2.28) in this expression gives

$$I = \frac{2e}{\hbar} \frac{\partial H}{\partial \varphi_1} = -\frac{2e}{\hbar} \frac{\partial H}{\partial \varphi_2}. \quad (2.30)$$

The phase difference is defined  $\Delta\varphi = \varphi_1 - \varphi_2$ , and as only the phase difference, not the individual phases, has physical meaning, we let  $\partial\varphi_1 \rightarrow \partial\Delta\varphi$  and  $\partial\varphi_2 \rightarrow -\partial\Delta\varphi$ . Hence

$$I = \frac{2e}{\hbar} \frac{\partial H}{\partial(\Delta\varphi)}. \quad (2.31)$$

Taking the expectation value of this gives

$$I = \frac{2e}{\hbar} \frac{\partial F}{\partial(\Delta\varphi)} \quad (2.32)$$

where  $F$  is the free energy, since

$$\frac{\partial F}{\partial(\Delta\varphi)} = -\frac{1}{\beta} \frac{1}{Z} \frac{\partial Z}{\partial(\Delta\varphi)} = -\frac{1}{\beta Z} \text{Tr} \left[ -\beta \frac{\partial H}{\partial(\Delta\varphi)} e^{-\beta H} \right] = \frac{1}{Z} \text{Tr} \left[ \frac{\partial H}{\partial(\Delta\varphi)} e^{-\beta H} \right] = \left\langle \frac{\partial H}{\partial(\Delta\varphi)} \right\rangle \quad (2.33)$$

with  $Z$  as the partition function:

$$Z = e^{-\beta F} = \text{Tr} \left[ e^{-\beta H} \right]. \quad (2.34)$$

This shows how the current is *phase-driven*. blablabla

## 2.5 Free Energy

The diagonal Hamiltonian in equation (2.10) is on the form as a free fermion gas:

$$\begin{aligned} H &= E_0 + \sum_{\mathbf{k}} \begin{pmatrix} \gamma_{\mathbf{k},\uparrow}^\dagger & \gamma_{-\mathbf{k},\downarrow} \end{pmatrix} \begin{pmatrix} E_{\mathbf{k}} & 0 \\ 0 & -E_{\mathbf{k}} \end{pmatrix} \begin{pmatrix} \gamma_{\mathbf{k},\uparrow} \\ \gamma_{-\mathbf{k},\downarrow}^\dagger \end{pmatrix} \\ &= E_0 + \sum_{\mathbf{k}} \left[ E_{\mathbf{k}} \gamma_{\mathbf{k},\uparrow}^\dagger \gamma_{\mathbf{k},\uparrow} - E_{\mathbf{k}} \left( 1 - \gamma_{-\mathbf{k},\downarrow}^\dagger \gamma_{-\mathbf{k},\downarrow} \right) \right] \\ &= E_0 + \sum_{\mathbf{k}} E_{\mathbf{k}} (N_{\uparrow} + N_{\downarrow} - 1) \end{aligned} \quad (2.35)$$

and the partition function of the system will be

$$\begin{aligned} Z &= \sum e^{-\beta H} = e^{-\beta E_0} \sum_{N_\uparrow, N_\downarrow} e^{-\beta \sum_k E_k (N_\uparrow + N_\downarrow - 1)} = e^{-\beta E_0} \prod_{\mathbf{k}} e^{\beta E_{\mathbf{k}}} \sum_{N_\uparrow} e^{-\beta E_{\mathbf{k}} N_\uparrow} \sum_{N_\downarrow} e^{-\beta E_{\mathbf{k}} N_\downarrow} \\ &= e^{-\beta E_0} \prod_{\mathbf{k}} e^{\beta E_{\mathbf{k}}} \left(1 + e^{-\beta E_{\mathbf{k}}}\right)^2 = e^{-\beta E_0} \prod_{\mathbf{k}} \left(2 \cosh\left(\frac{\beta E_{\mathbf{k}}}{2}\right)\right)^2 \end{aligned} \quad (2.36)$$

This expression may now be used to find the free energy of the system:

$$F = -\frac{1}{\beta} \ln(Z) = E_0 - 2k_B T \sum_{\mathbf{k}} \ln \left[ 2 \cosh\left(\frac{E_{\mathbf{k}}}{2k_B T}\right) \right]. \quad (2.37)$$

# Chapter 3

## Physical System

We consider a two-dimensional SNS-junction in the  $xy$ -plane and parallel to the  $x$ -axis, with the interfaces placed at  $x = -L/2$  and  $x = L/2$ . The width of the junction is  $W$ , see figure 3.1. The quasiparticle waves are represented by the four-component vectors  $\Psi(x, y) = (\vec{u}(x, y) \ \vec{v}(x, y))^T$  as used in the Bogoliubov equations (2.25). We consider s-wave superconductors such that the gap parameter,  $\Delta(x)$ , is position-independent in each superconductor. The left and right superconductors are assumed to be of the same material, so that the magnitude,  $\Delta_0$ , of the gap parameter is the same in both superconductors. However, we allow the gap parameter to have different phases,  $\phi_L$  and  $\phi_R$ , in the left and right superconductor, respectively. Necessarily, the gap parameter is zero in the normal metal. The overall gap parameter is

$$\Delta(x) = \Delta_0 \left( e^{i\phi_L} \Theta(-L/2 - x) + e^{i\phi_R} \Theta(x - L/2) \right), \quad (3.1)$$

where  $\Theta(x)$  is the Heaviside step function. The Hamiltonian will be on the form given in equation (2.20). We allow for different chemical potential,  $\mu_S$  and  $\mu_N$ , but we assume the effective mass to be equal in the superconductor and the normal metal, i.e.  $m_S = m_N \equiv m$ . Moreover, we let  $V(x)$  be a delta-potential barrier at the interfaces and allow for different strength, i.e.  $V(x) = V_L \delta(x + L/2) + V_R \delta(x - L/2)$ . The overall Hamiltonian is

$$h(x, y) = h_S(x, y) (\Theta(-L/2 - x) + \Theta(x - L/2)) + h_N(x, y) \Theta(x + L/2) \Theta(L/2 - x) + V_L \delta(x) + V_R \delta(x - L) \quad (3.2)$$

where the Hamiltonian in the superconductors (S) and normal metal (N) is given as

$$h_{S/N}(x, y) = \frac{1}{2m} (-i\hbar\nabla - q\mathbf{A}(x, y))^2 - \mu_{S/N} \quad (3.3)$$

and  $\mathbf{A}$  is the vector potential allowing for an external magnetic field.

We will consider the semiclassical limit  $k_F L \gg 1$ , in which the Andreev bound states can be associated with classical trajectories, as illustrated in figure 3.1. These trajectories can be thought of as single-mode waveguides connecting the two superconductors !!!REF!!!. We will focus the circular Fermi surface with isotropic dependence on the wave vector  $\mathbf{k} = (k_x, k_y) = (k_F \cos \theta_k, k_F \sin \theta_k)$ . We will work in the short-junction regime  $L \ll \xi$ , with  $\xi = \hbar v_f / \Delta$  the superconducting coherence length induced by the proximity effect !!!CITE!!!.

In the preceding chapters we will look at three different situations. First, in section 4.1 and 5.1, we will consider the system without external field or barriers at the interfaces. Next, in section 4.2 and 5.2, we will include the barriers at each interface, but keep the external field off. Finally, in section 4.3 and 5.3, we will include an external field, but have transparent barriers. The situations without the external field is well known !!!REF!!! and will be used for comparison. There has also been research on the situation with a uniform external magnetic field, both for one-dimensional and two-dimensional systems !!!REF!!!. However, we will also consider modulated magnetic fields, which has not yet been explored. Our strategy in all three situations is to first find the ABS-energies (chapter 4) and use this result to find the Josephson current (chapter 5).

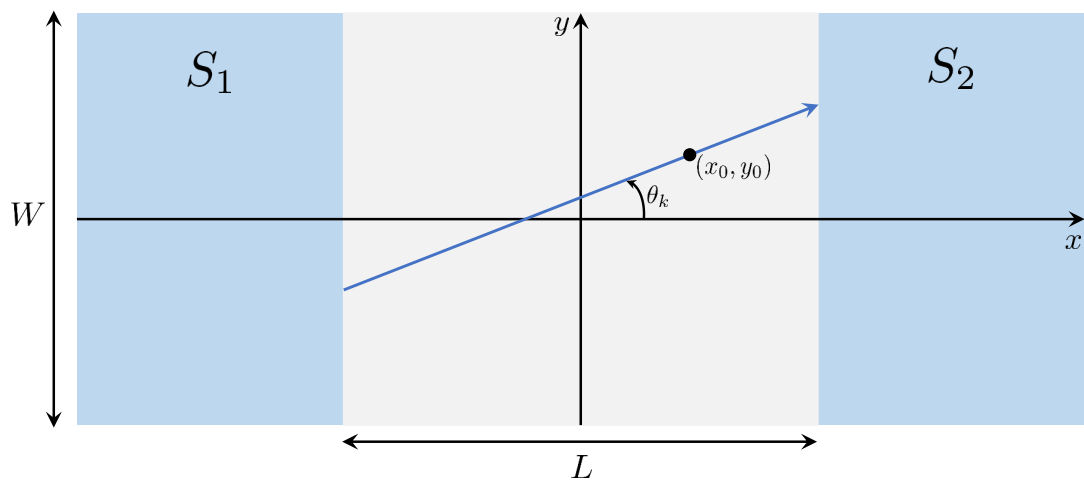


Figure 3.1: blabla

# **Chapter 4**

## **Andreev Bound State energies in SNS-junction**

We will in this chapter find the ABS energies in the three situations described in chapter 3. For the situations without barriers at the interfaces the Andreev bound states will accumulate phase shifts as it travels along the classical trajectory described in chapter 3. This allow us to use the Bohr-Sommerfeld quantization condition !!!CITE!!! to find the ABS energies. When we include barriers the Andreev reflections can not be expressed as phase shifts and we must find the energies by setting up the wave-functions in each region and use boundary conditions to solve the system.

### **4.1 ABS energies without barriers or applied field**

We will first consider the system with no applied field ( $A = 0$ ) and no barriers ( $V_L = V_R = 0$ ). We will first find the phase shift accumulated over a penetration depth in the superconductor when an electron or a hole is Andreev reflected at the NS-interface. Adding this to the phase accumulated when the electron or hole is traveling along the trajectory in figure 3.1, the total phase shift of the Andreev bound state is found and the Bohr-Sommerfeld quantization condition can be used to find the energies.

### 4.1.1 Andreev reflection amplitude

The probability amplitudes from chapter section 2.3 may be found by using the boundary conditions at the interface between the normal metal and the super conductor. With no barriers the boundary conditions yields

$$\begin{aligned}\psi_i(0, y) + \psi_r(0, y) &= \psi_t(0, y) \\ \frac{\partial}{\partial x} \psi_i(0, y) + \frac{\partial}{\partial x} \psi_r(0, y) &= \frac{\partial}{\partial x} \psi_t(0, y).\end{aligned}\tag{4.1}$$

We insert the wave functions given in equation (??) in the boundary conditions and solve the system. The resulting amplitudes are given as

$$\begin{aligned}r_{eh} &= \frac{2e^{-i\varphi}}{\frac{u_0}{v_0} \frac{k_x^- + q_x^-}{k_x^+ + k_x^-} \left(1 + \frac{k_x^+}{q_x^+}\right) + \frac{v_0}{u_0} \frac{k_x^+ - q_x^-}{k_x^+ + k_x^-} \left(1 - \frac{k_x^-}{k_x^+}\right)} \\ r_{ee} &= \left( \frac{u_0}{v_0} \frac{k_x^+ + q_x^-}{k_x^+ + k_x^-} + \frac{v_0}{u_0} \frac{k_x^+ - q_x^-}{k_x^+ + k_x^-} \right) e^{i\varphi} r_{eh} \\ t_{ee} &= \frac{1}{v_0} \frac{k_x^- + q_x^-}{k_x^+ + k_x^-} e^{-i\beta} r_{eh} \\ t_{eh} &= \frac{1}{u_0} \frac{k_x^+ - q_x^-}{k_x^+ + k_x^-} e^{i\alpha} r_{eh},\end{aligned}\tag{4.2}$$

where  $\varphi = \alpha - \beta$  is the phase of the gap parameter as shown in section 2.2.3. Since we are considering Andreev Bound States we are especially interested in the  $r_{eh}$ -amplitude, and see that it's expression may be simplified in the Andreev approximation !!!CITE!!! in which we let  $k_x^\pm \approx q_x^\pm$ :

$$r_{eh} = \frac{v_0}{u_0} e^{-i\varphi} \equiv e^{-i\eta} e^{-i\varphi},\tag{4.3}$$

where  $\eta$  is as defined in equation (2.18). Similarly, the amplitude of an incoming hole which is Andreev reflected as an electron will be  $r_{he} = r_{eh}^*$ :

$$r_{he} = \frac{v_0}{u_0} e^{i\varphi} = e^{-i\eta} e^{i\varphi}.\tag{4.4}$$

Hence, the Andreev reflection give a phase shift of  $-\eta \mp \varphi$ , where we use the upper (lower) sign if the incoming particle is an electron (hole) .

### 4.1.2 Bohr-Sommerfeld quantization

In the short junction regime, the continuous quasiparticle excitation spectrum ( $E_{\mathbf{k}} < \Delta_0$ ) will not contribute to the Josephson current !!!CITE!!! and it is sufficient to restrict our selves to energies below the gap  $E_{\mathbf{k}} < \Delta_0$  which yields  $\eta = \arccos(E_{\mathbf{k}}/\Delta_0)$ , according to equation(2.18). The Bohr-Sommerfeld quantization condition require the total phase obtained by the state in a whole cycle to be a multiple of  $2\pi$ . REFERANSE. An electron starting at the left interface traveling towards the right interface along a trajectory at an angle  $\theta$ , see figure 3.1, would gain a phase of  $L(k_x^+ + k_y^+ \tan \theta)$ , before it is Andreev reflected at the right interface with the amplitude  $r_{eh}$  and thus is gaining a phase of  $-\eta - \varphi$ . The state would then continue as a hole traveling back along the same trajectory, accumulating a phase of  $-L(k_x^- + k_y^- \tan \theta)$ . Hence, the total phase in the quantization condition yields

$$\begin{aligned} 2\pi n = \oint d\phi &= \int_L^R \pm \mathbf{k}^\pm \cdot d\mathbf{l} + \phi_{(eh)(he)}^R + \int_R^L \pm \mathbf{k}^\mp \cdot d\mathbf{l} + \phi_{(he)(eh)}^L \\ &= L(k_x^+ - k_x^-) + L \tan \theta (k_y^+ - k_y^-) - 2\eta \pm \Delta\varphi \end{aligned} \quad (4.5)$$

where  $\phi_{(eh)(he)}^{R/L} = -\eta \mp \varphi_{R/L}$  is the phase from Andreev reflection of a electron (hole) and we have defined the phase difference  $\Delta\varphi \equiv \varphi_L - \varphi_R$ . The upper sign indicate that the state starts out as a right-going electron, while the lower sign indicate that it starts as a right-going hole. Again we use the Andreev approximation and let  $k_x^+ \approx k_x^-$  and  $k_y^+ \approx k_y^-$  such that the two first terms vanish and the quantization condition is simply

$$2\pi n = -2\eta \pm \Delta\varphi. \quad (4.6)$$

### 4.1.3 ABS energy

Inserting equation (2.18) in the quantization condition above (4.6) we find the Andreev energy levels

$$E_{\mathbf{k}} = \Delta_0 \cos \eta = \Delta_0 \cos \left( \frac{\Delta \varphi}{2} \right). \quad (4.7)$$

This is the well known result in a SNS Josephson junction !!!CITE!!!.

## 4.2 ABS energies with barriers

We will in this section allow for barriers. Then the Andreev reflection amplitude will be more complicated so that we can not express it as a phase shift like we did above. We will instead find the energies by setting up the wave-functions in each region, insert the wave-functions in the boundary conditions and solve the system. The Hamiltonian of the system will be as given in equation (3.2), but with no external field so that we can set  $\mathbf{A}$  to zero. Hence,

$$h_{S/N}(x, y) = -\hbar^2 \nabla^2 / 2m - \mu_{S/N}. \quad (4.8)$$

### 4.2.1 Boundary conditions

Charge conservation yields continuous wave-functions at the interfaces:

$$\begin{aligned} \Psi_L(-L/2, y) &= \Psi_N(-L/2, y) \equiv \Psi(-L/2, y), \\ \Psi_R(L/2, y) &= \Psi_N(L/2, y) \equiv \Psi(L/2, y). \end{aligned} \quad (4.9)$$

We find the boundary conditions for the derivatives by integrating the BdG-equations (2.25):

$$\begin{aligned}
0 &= \lim_{\epsilon \rightarrow 0} \int_{-L/2-\epsilon}^{-L/2+\epsilon} E_{\mathbf{k}} \Psi(x, y) dx = \lim_{\epsilon \rightarrow 0} \int_{-L/2-\epsilon}^{-L/2+\epsilon} \begin{pmatrix} \hat{H}(x, y) & \hat{\Delta}(x) \\ \hat{\Delta}^\dagger(x) & -\hat{H}(x, y) \end{pmatrix} \Psi(x, y) dx \\
&= \lim_{\epsilon \rightarrow 0} \int_{-L/2-\epsilon}^{-L/2^-} \begin{pmatrix} h_S(x, y) \hat{\sigma}_0 & i\Delta(x) \hat{\sigma}_2 \\ -i\Delta^*(x) \hat{\sigma}_2 & -h_S(x, y) \hat{\sigma}_0 \end{pmatrix} \Psi_L(x, y) dx + \begin{pmatrix} V_L \hat{\sigma}_0 & 0 \\ 0 & -V_L \hat{\sigma}_0 \end{pmatrix} \Psi(-L/2, y) \\
&\quad + \lim_{\epsilon \rightarrow 0} \int_{-L/2^+}^{-L/2+\epsilon} \begin{pmatrix} h_N(x) \hat{\sigma}_0 & 0 \\ 0 & -h_S(x) \hat{\sigma}_0 \end{pmatrix} \Psi_N(x, y) dx \\
&= \begin{pmatrix} \hat{\sigma}_0 & 0 \\ 0 & -\hat{\sigma}_0 \end{pmatrix} \left( V_L \Psi(-L/2, y) - \frac{\hbar^2}{2m} \lim_{\epsilon \rightarrow 0} \left( \int_{-L/2-\epsilon}^{-L/2^-} \frac{\partial^2}{\partial x^2} \Psi_L(x, y) dx + \int_{-L/2^+}^{-L/2+\epsilon} \frac{\partial^2}{\partial x^2} \Psi_N(x, y) dx \right) \right) \\
&= \begin{pmatrix} \hat{\sigma}_0 & 0 \\ 0 & -\hat{\sigma}_0 \end{pmatrix} \left( V_L \Psi(-L/2, y) - \frac{\hbar^2}{2m} \left( \frac{\partial \Psi_N}{\partial x} \Big|_{x=-L/2} - \frac{\partial \Psi_L}{\partial x} \Big|_{x=-L/2} \right) \right),
\end{aligned}$$

and the boundary condition at the left interface for the derivatives is thus

$$\frac{\partial \Psi_N}{\partial x} \Big|_{x=-L/2} - \frac{\partial \Psi_L}{\partial x} \Big|_{x=-L/2} = \frac{2m}{\hbar^2} V_L \Psi(-L/2, y). \quad (4.10)$$

Similarly, we get

$$\frac{\partial \Psi_R}{\partial x} \Big|_{x=L/2} - \frac{\partial \Psi_N}{\partial x} \Big|_{x=L/2} = \frac{2m}{\hbar^2} V_R \Psi(L/2, y). \quad (4.11)$$

as boundary condition at the right interface.

### 4.2.2 Wave functions in the superconduction region

The solution of the BdG-equations (2.25) that satisfy the boundary conditions will be on the form

$$\Psi_{\mathbf{k}^\pm}(\mathbf{r}) = \begin{pmatrix} \vec{u}_{\mathbf{k}} \\ \vec{v}_{\mathbf{k}} \end{pmatrix} e^{i\mathbf{k}^\pm \cdot \mathbf{r}}. \quad (4.12)$$

Inserting the wavefunctions of this form in the time-independent Schrödinger equation yields

$$h(\mathbf{r}) \Psi_{\mathbf{k}^\pm}(\mathbf{r}) = \left( \frac{\hbar^2 k^{\pm 2}}{2m} - \mu \right) \Psi_{\mathbf{k}^\pm}(\mathbf{r}) \equiv \varepsilon_k^\pm \Psi_{\mathbf{k}^\pm}(\mathbf{r}), \quad (4.13)$$

where we let  $h(\mathbf{r}) = h_S(x, y)$  as given in (4.8) in the superconducting region. For the eigenvalue problem in the BdG-equations (2.25) we must calculate

$$\begin{aligned} 0 &= \det \begin{pmatrix} (\varepsilon_{\mathbf{k}}^{\pm} - E_{\mathbf{k}}) \hat{\sigma}_0 & i\Delta \hat{\sigma}_2 \\ -i\Delta^* \hat{\sigma}_2 & (-\varepsilon_{\mathbf{k}}^{\pm} - E_{\mathbf{k}}) \hat{\sigma}_0 \end{pmatrix} \\ &= (\varepsilon_{\mathbf{k}}^{\pm} - E_{\mathbf{k}})^2 \left( \varepsilon_{\mathbf{k}}^{\pm} + E_{\mathbf{k}} + \frac{\Delta_0^2}{\varepsilon_{\mathbf{k}}^{\pm} - E_{\mathbf{k}}} \right)^2. \end{aligned} \quad (4.14)$$

As  $E_{\mathbf{k}} = \varepsilon_{\mathbf{k}}^{\pm}$  would give zero in the denominator when  $\Delta_0$  is non-zero, the only solution to the above equation (4.14) is

$$E_{\mathbf{k}}^2 = \varepsilon_{\mathbf{k}}^{\pm 2} + \Delta_0^2 \quad (4.15)$$

which agrees with the energies obtained in equation (2.16).  $k^{\pm}$  and  $\varepsilon_{\mathbf{k}}^{\pm}$  will be as in equation (2.17) and we will only consider positive energies,  $E_{\mathbf{k}} = \sqrt{\varepsilon_{\mathbf{k}}^{\pm 2} + \Delta_0^2}$ . For  $\varepsilon_{\mathbf{k}}^+ = +\sqrt{E_{\mathbf{k}}^2 - \Delta_0^2} = i\Delta_0 \sin \eta$  we get the (non-normalized) wave-functions describing electronlike quasiparticles:

$$\Psi_{e,\uparrow}^{\pm}(x, y) = \begin{pmatrix} e^{i(\eta+\varphi)} \\ 0 \\ 0 \\ 1 \end{pmatrix} e^{i(\pm k_x^+ x + k_y^+ y)} \quad \text{and} \quad \Psi_{e,\downarrow}^{\pm}(x, y) = \begin{pmatrix} 0 \\ e^{i(\eta+\varphi)} \\ -1 \\ 0 \end{pmatrix} e^{i(\pm k_x^+ x + k_y^+ y)}, \quad (4.16)$$

where  $\Psi_{e,\sigma}^+$  are right-going waves, while  $\Psi_{e,\sigma}^-$  are left-going waves. Similarly, for  $\varepsilon_{\mathbf{k}}^- = -\sqrt{E_{\mathbf{k}}^2 - \Delta_0^2} = -i\Delta_0 \sin \eta$  we get the wave-functions describing holelike quasiparticles:

$$\Psi_{h,\uparrow}^{\pm}(x, y) = \begin{pmatrix} 1 \\ 0 \\ 0 \\ e^{i(\eta-\varphi)} \end{pmatrix} e^{i(\pm k_x^- x + k_y^- y)} \quad \text{and} \quad \Psi_{h,\downarrow}^{\pm}(x, y) = \begin{pmatrix} 0 \\ -1 \\ e^{i(\eta-\varphi)} \\ 0 \end{pmatrix} e^{i(\pm k_x^- x + k_y^- y)}, \quad (4.17)$$

where  $\Psi_{h,\sigma}^+$  are left-going waves, while  $\Psi_{h,\sigma}^-$  are right-going waves. The direction of the waves is determined from the group velocity:

$$\mathbf{v}_g = \frac{1}{\hbar} \frac{\partial E_{\mathbf{k}}}{\partial \mathbf{k}} = \frac{\varepsilon_{\mathbf{k}}^{\pm}}{E_{\mathbf{k}}} \frac{\hbar \mathbf{k}^{\pm}}{m}. \quad (4.18)$$

We allow for different phases,  $\varphi_L$  and  $\varphi_R$ , in each region. As we will only consider energies below the gap,  $E_{\mathbf{k}} < \Delta_0$ , the wave vectors (2.17) will get imaginary parts and must vanish in the superconductors. Consequently there will be no incoming wave-functions from the superconductor into the normal metal with such energies and we need only to consider the outgoing wave-functions in the superconducting regions. We let  $k_y^+ \approx k_y^- \equiv k_y$  and the total wave functions in the left (L) and right (R) region will thus be

$$\begin{aligned}\Psi_L(x - L/2, y) &= \Psi_L(x - L/2) e^{ik_y y} \\ \Psi_R(x + L/2, y) &= \Psi_R(x + L/2) e^{ik_y y}\end{aligned}\tag{4.19}$$

with  $\Psi_{L/R}(x \mp L/2)$  defined as

$$\begin{aligned}\Psi_L(x - L/2) &= a_1 \begin{pmatrix} e^{i(\eta+\varphi_L)} \\ 0 \\ 0 \\ 1 \end{pmatrix} e^{-ik_x^+ x} + a_2 \begin{pmatrix} 0 \\ e^{i(\eta+\varphi_L)} \\ -1 \\ 0 \end{pmatrix} e^{-ik_x^+ x} + a_3 \begin{pmatrix} 1 \\ 0 \\ 0 \\ e^{i(\eta-\varphi_L)} \end{pmatrix} e^{ik_x^- x} + a_4 \begin{pmatrix} 0 \\ -1 \\ e^{i(\eta-\varphi_L)} \\ 0 \end{pmatrix} e^{ik_x^- x} \\ \Psi_R(x + L/2) &= b_1 \begin{pmatrix} e^{i(\eta+\varphi_R)} \\ 0 \\ 0 \\ 1 \end{pmatrix} e^{ik_x^+ x} + b_2 \begin{pmatrix} 0 \\ e^{i(\eta+\varphi_R)} \\ -1 \\ 0 \end{pmatrix} e^{ik_x^+ x} + b_3 \begin{pmatrix} 1 \\ 0 \\ 0 \\ e^{i(\eta-\varphi_R)} \end{pmatrix} e^{-ik_x^- x} + b_4 \begin{pmatrix} 0 \\ -1 \\ e^{i(\eta-\varphi_R)} \\ 0 \end{pmatrix} e^{-ik_x^- x}.\end{aligned}\tag{4.20}$$

We have here absorbed a phase factor  $\exp(\pm ik_x L/2)$  in the coefficients in order to simplify the boundary equations.

### 4.2.3 Wave functions in the normal region

In the normal region the gap parameter,  $\Delta(x)$ , is zero, and so  $u_0 = 1$  and  $v_0 = 0$  and the eigenvalues are  $E_k$  such that  $\epsilon_k^\pm = \pm E_k$ . The corresponding eigenvectors are

$$\Psi_{e,\uparrow}(\mathbf{r}) = \begin{pmatrix} 1 \\ 0 \\ 0 \\ 0 \end{pmatrix} e^{i\mathbf{k}^+ \cdot \mathbf{r}}, \quad \Psi_{e,\downarrow}(\mathbf{r}) = \begin{pmatrix} 0 \\ 1 \\ 0 \\ 0 \end{pmatrix} e^{i\mathbf{k}^+ \cdot \mathbf{r}}, \quad \Psi_{h,\uparrow}(\mathbf{r}) = \begin{pmatrix} 0 \\ 0 \\ 1 \\ 0 \end{pmatrix} e^{i\mathbf{k}^- \cdot \mathbf{r}}, \quad \Psi_{h,\downarrow}(\mathbf{r}) = \begin{pmatrix} 0 \\ 0 \\ 0 \\ 1 \end{pmatrix} e^{i\mathbf{k}^- \cdot \mathbf{r}}. \quad (4.21)$$

We must here allow both right- and leftgoing waves and the total wave function in the normal region becomes

$$\Psi_N(x - L/2, y) = \Psi_N(x - L/2) e^{ik_y y} \quad (4.22)$$

with

$$\begin{aligned} \Psi_N(x - L/2) = & c_1 \begin{pmatrix} 1 \\ 0 \\ 0 \\ 0 \end{pmatrix} e^{ik^+ x} + c_2 \begin{pmatrix} 1 \\ 0 \\ 0 \\ 0 \end{pmatrix} e^{-ik^+ x} + c_3 \begin{pmatrix} 0 \\ 1 \\ 0 \\ 0 \end{pmatrix} e^{ik^+ x} + c_4 \begin{pmatrix} 0 \\ 1 \\ 0 \\ 0 \end{pmatrix} e^{-ik^+ x} \\ & + c_5 \begin{pmatrix} 0 \\ 0 \\ 1 \\ 0 \end{pmatrix} e^{ik^- x} + c_6 \begin{pmatrix} 0 \\ 0 \\ 1 \\ 0 \end{pmatrix} e^{-ik^- x} + c_7 \begin{pmatrix} 0 \\ 0 \\ 0 \\ 1 \end{pmatrix} e^{ik^- x} + c_8 \begin{pmatrix} 0 \\ 0 \\ 0 \\ 1 \end{pmatrix} e^{-ik^- x}. \end{aligned} \quad (4.23)$$

### 4.2.4 ABS energy

We use the boundary conditions found in section 4.2.1:

$$\begin{aligned} \Psi_L(-L/2) - \Psi_N(-L/2) &= 0 \\ \Psi_R(L/2) - \Psi_N(L/2) &= 0 \\ \frac{\partial \Psi_N(x)}{\partial x} \Big|_{x=-L/2} - \frac{\partial \Psi_L(x)}{\partial x} \Big|_{x=-L/2} - Z_L k_x \Psi_L(-L/2) &= 0 \\ \frac{\partial \Psi_R(x)}{\partial x} \Big|_{x=L/2} - \frac{\partial \Psi_N(x)}{\partial x} \Big|_{x=L/2} - Z_R k_x \Psi_R(L/2) &= 0 \end{aligned} \quad (4.24)$$

and insert the equations in a homogeneous matrix equation of the form

$$M(a_1 \cdots a_4 \ b_1 \cdots b_4 \ c_1 \cdots c_8)^T = 0 \quad (4.25)$$

where  $M$  is a  $16 \times 16$ -matrix. We have let  $k_x^+ \approx k_x^- \equiv k_x$  and defined the barrier strengths

$$Z_L = \frac{2mV_L}{\hbar^2 k_x^2} \quad \text{and} \quad Z_R = \frac{2mV_R}{\hbar^2 k_x^2}. \quad (4.26)$$

The determinant of  $M$  is found to be

$$\det(M) = \left(8e^{i\eta}\right)^4 \left[ \sin^2 \frac{\Delta\varphi}{2} - (1 + \zeta) \sin^2 \eta \right]^2 \quad (4.27)$$

which must be zero in order for the equations to have non-trivial solutions. Hence, the energy is

$$E = \Delta_0 \cos \eta = \Delta_0 \sqrt{\frac{\cos^2 \frac{\Delta\varphi}{2} + \zeta}{\zeta + 1}}. \quad (4.28)$$

We have again let  $\Delta\varphi = \varphi_L - \varphi_R$  be the phase difference between the left and right semiconductor. We have also introduced  $\zeta$  which measures the effect of the barriers and is given as

$$\zeta = Z^2 + z^2 \sin(k_F L) \left[ Z \cos(k_F L) + \left( \frac{z^2}{4} - 1 \right) \sin(k_F L) \right] \quad (4.29)$$

where  $Z$  and  $z$  are defined as

$$Z = \frac{Z_L + Z_R}{2} \quad \text{and} \quad z = \sqrt{Z_L Z_R}. \quad (4.30)$$

In the limit with no barrier, i.e.  $\zeta = 0$  we see that equation (4.28) yields (4.7).

### 4.3 ABS energies with applied field

We will now apply a magnetic field,  $\vec{B}$ , to the junction, and let the barriers be transparent. This imply modifying the Hamiltonian to

$$h_N(\mathbf{r}) = \frac{1}{2m_N} \left( \frac{\hbar}{i} \nabla - q\mathbf{A}(\mathbf{r}) \right)^2 + q\varphi - \mu_N \quad (4.31)$$

with  $\mathbf{A}(\mathbf{r})$  as the vector potential and  $\varphi$  as the scalar potential.

Our strategy now is the same as in section 4.1. We want to express the problem in the phase of the wave function and use the quantization condition to find the energy.

#### 4.3.1 Guage transformation

As we must have Gauge invariance we may do the transformation

$$\begin{aligned} \mathbf{A}' &= \mathbf{A} + \nabla f \\ \varphi' &= \varphi - \frac{\partial f}{\partial t} \end{aligned} \quad (4.32)$$

where  $f$  is any function of position and time. Doing such transformation imply a transformation in the wavefunction  $\Psi$  as well. Considering the time-dependent Schrödinger equation yields

$$\begin{aligned} i\hbar \frac{\partial \Psi}{\partial t} &= \left[ \frac{1}{2m} \left( \frac{\hbar}{i} \nabla - q\mathbf{A}' \right)^2 + q\varphi' - \mu_N \right] \Psi \\ &= \left[ \frac{1}{2m} \left( \frac{\hbar}{i} \nabla - q\mathbf{A}' + q\nabla f \right)^2 + q\varphi' + q \frac{\partial f}{\partial t} - \mu_N \right] \Psi, \end{aligned} \quad (4.33)$$

giving

$$i\hbar \frac{\partial \Psi}{\partial t} - q \frac{\partial f}{\partial t} \Psi = \left[ \frac{1}{2m} \left( \frac{\hbar}{i} \nabla - q\mathbf{A}' + q\nabla f \right)^2 + q\varphi' - \mu_N \right] \Psi \quad (4.34)$$

or

$$\begin{aligned} i\hbar \frac{\partial}{\partial t} \left( \Psi e^{iqf/\hbar} \right) &= e^{iqf/\hbar} \left[ \frac{1}{2m} \left( \frac{\hbar}{i} \nabla - q\mathbf{A}' + q\nabla f \right)^2 + q\varphi' \right] \Psi \\ &= \left[ \frac{1}{2m} \left( \frac{\hbar}{i} \nabla - q\mathbf{A}' \right)^2 + q\varphi' \right] \left( \Psi e^{iqf/\hbar} \right), \end{aligned} \quad (4.35)$$

where we have used that

$$e^{iqf/\hbar} \left( \frac{\hbar}{i} \nabla + q \nabla f \right) \Psi = \frac{\hbar}{i} \nabla \left( e^{iqf/\hbar} \Psi \right). \quad (4.36)$$

The Schrödinger equation in the transformed system is now on the same form as the original system:

$$i\hbar \frac{\partial \Psi'}{\partial t} = \left[ \frac{1}{2m} \left( \frac{\hbar}{i} \nabla - q \mathbf{A}' \right)^2 + q\varphi' \right] \Psi' \quad (4.37)$$

with  $\Psi' = e^{iqf/\hbar} \Psi$ . Thus a Gauge transformation  $\mathbf{A} \rightarrow \mathbf{A} + \nabla \chi$  imply a transformation  $\phi \rightarrow \phi + q\chi/\hbar$  in the phase.

A Gauge invariant phase will be on the form

$$\phi_{GI} = \phi - \frac{q}{\hbar} \int \mathbf{A} \cdot d\mathbf{r}, \quad (4.38)$$

as transformation  $\phi \rightarrow \phi + q\chi/\hbar$  and  $\mathbf{A} \rightarrow \mathbf{A} + \nabla \chi$  give

$$\begin{aligned} \phi_{GI} &\rightarrow \phi + \frac{q}{\hbar} \chi - \frac{q}{\hbar} \int (\mathbf{A} + \nabla \chi) \cdot d\mathbf{r} = \phi - \frac{q}{\hbar} \int \mathbf{A} \cdot d\mathbf{r} + \frac{q}{\hbar} \chi - \frac{q}{\hbar} \chi \\ &= \phi - \frac{q}{\hbar} \int \mathbf{A} \cdot d\mathbf{r}. \end{aligned} \quad (4.39)$$

We have in the previous sections taken  $\mathbf{A}$  to be zero so that  $\phi_{GI} = \phi$ . However, now we must include the vector potential in the phase as the magnetic field is non-zero.

### 4.3.2 Bohr-Sommerfeld quantization condition

Using the same method as in equation (4.6), but with the Gauge invariant phase we get the quantization condition

$$\begin{aligned} 2\pi n &= \oint d\phi = \int_L^R \pm \mathbf{k}^\pm \cdot d\mathbf{l} \pm \frac{e}{\hbar} \int_L^R \mathbf{A} \cdot d\mathbf{l} + \phi_{(eh)(he)}^R + \int_R^L \pm \mathbf{k}^\mp \cdot d\mathbf{l} \mp \frac{e}{\hbar} \int_R^L \mathbf{A} \cdot d\mathbf{l} + \phi_{(he)(eh)}^L \\ &= L(k_x^+ - k_x^-) + L \tan \theta (k_y^+ - k_y^-) - 2\eta \pm \left( \Delta\varphi + \frac{2e}{\hbar} \int_L^R \mathbf{A} \cdot d\mathbf{l} \right). \end{aligned} \quad (4.40)$$

Again, we let  $k_x^+ \approx k_x^-$  and  $k_y^+ \approx k_y^-$  and are left with

$$2\pi n = -2\eta \pm (\Delta\varphi - \gamma), \quad (4.41)$$

where we have defined

$$\gamma = -\frac{2e}{\hbar} \int_L^R \mathbf{A} \cdot d\mathbf{l}. \quad (4.42)$$

We have assumed the curvature of the electrons, due to the Lorentz force, to be much larger than the length of the junction, so that we can neglect the effect the field has on the trajectory of the electrons/holes.

### 4.3.3 ABS energy

The energy is then

$$E_{\mathbf{k}} = \Delta_0 \cos \eta = \Delta_0 \cos \left( \frac{\Delta\varphi}{2} - \frac{\gamma}{2} \right). \quad (4.43)$$

We see that when the the field is zero, i.e.  $\gamma = 0$ , we get the same expression as equation (4.7).

# Chapter 5

## Andreev Bound State Current in SNS-junction

In chapter 2.4 we saw how the Josephson current can be expressed in terms of the free energy and phase difference between the two superconductors (2.32). In chapter 2.5 we expressed the free energy in terms of the energy levels,  $E_{\mathbf{k}}$ . Using equation (2.32) and (2.37) we can thus express the Josephson current in terms of the ABS energy and the phase difference:

$$\begin{aligned} I_x(\Delta\varphi) &= \sum_{k_y} \delta I(\mathbf{r}, \mathbf{k}) \rightarrow \int dy \int \frac{dk_y}{2\pi} \delta I(\mathbf{r}, \mathbf{k}), \\ I_y(\Delta\varphi) &= \sum_{k_x} \delta I(\mathbf{r}, \mathbf{k}) \rightarrow \int dx \int \frac{dk_x}{2\pi} \delta I(\mathbf{r}, \mathbf{k}), \end{aligned} \quad (5.1)$$

where we have defined

$$\delta I(\mathbf{r}, \mathbf{k}) \equiv -\frac{2e}{\hbar} \tanh\left(\frac{E_{\mathbf{k}}}{2k_B T}\right) \frac{\partial E_{\mathbf{k}}}{\partial(\Delta\varphi)} \quad (5.2)$$

and  $I_y$  should be zero due to current conservation. The current density will be given as

$$\begin{aligned} j_x(x, y) &= \int \frac{dk_y}{2\pi} \delta I(\mathbf{r}, \mathbf{k}) = \frac{k_F}{2\pi} \int_{-\pi/2}^{\pi/2} d\theta_k \cos\theta_k \delta I(\mathbf{r}, \mathbf{k}), \\ j_y(x, y) &= \int \frac{dk_x}{2\pi} \delta I(\mathbf{r}, \mathbf{k}) = \frac{k_F}{2\pi} \int_{-\pi/2}^{\pi/2} d\theta_k \sin\theta_k \delta I(\mathbf{r}, \mathbf{k}), \end{aligned} \quad (5.3)$$

where we have let

$$\begin{pmatrix} dk_x \\ dk_y \end{pmatrix} \rightarrow k_F \begin{pmatrix} \sin \theta_k \\ \cos \theta_k \end{pmatrix} d\theta_k \quad (5.4)$$

as we consider the circular Fermi surface, as stated in chapter 3.

In chapter 4 the ABS energy levels were found for the three different situations and we will in this chapter use these energies in equation (5.3) to find the current density and in equation (5.6) to find the total and critical current for each of the three situations. For the analytical progress we will consider the high temperature regime, ( $k_B T \gtrsim \Delta_0$ ), in which the analytical calculations are simpler.

## 5.1 ABS current without barriers or applied field

In the case with no barriers or magnetic field we use equation (4.7) in equation (5.2) to obtain

$$\delta I = \frac{e\Delta_0}{\hbar} \sin\left(\frac{\Delta\varphi}{2}\right) \tanh\left(\frac{\Delta_0 \cos(\Delta\varphi/2)}{2k_B T}\right), \quad (5.5)$$

which we notice is independent of the trajectory of the particle. From equation (5.3) one finds the current density to be zero in the  $y$ -direction,  $j_y(x, y) = 0$ , and uniform in the  $x$ -direction,  $j_x(x, y) = I_x/W$ , where  $W$  is the junction width (indicated in figure 3.1) and  $I_x$  as the total current:

$$I_x = k_F W \frac{e\Delta_0}{\pi\hbar} \sin\left(\frac{\Delta\varphi}{2}\right) \tanh\left(\frac{\Delta_0 \cos(\Delta\varphi/2)}{2k_B T}\right). \quad (5.6)$$

In the high temperature regime ( $k_B T \gtrsim \Delta_0$ ) this can be approximated to

$$I_x = k_F W \frac{e\Delta_0}{\pi\hbar} \sin\left(\frac{\Delta\varphi}{2}\right) \frac{\Delta_0 \cos(\Delta\varphi/2)}{2k_B T} = I_{c,0} \sin \Delta\varphi \quad (5.7)$$

with

$$I_{c,0} = \frac{k_F W e \Delta_0^2}{4\pi\hbar k_B T} \quad (5.8)$$

as the high temperature critical current. These results are well known !!!CITE!!! and will be used for comparison in the preceding sections.

## 5.2 ABS current with barriers

The ABS energy levels in the case of no barriers was found in equation (4.28). Inserting this in equation (5.2) yields

$$\delta I = \frac{e\Delta_0}{2\hbar} \frac{\sin(\Delta\varphi)}{\sqrt{(\cos^2(\Delta\varphi/2) + \zeta)(\zeta + 1)}} \tanh\left(\frac{\Delta_0}{2k_B T} \sqrt{\frac{\cos^2(\Delta\varphi/2) + \zeta}{\zeta + 1}}\right). \quad (5.9)$$

Also here  $\delta I$  is independent of the trajectory such that the current density is uniform. The total current is

$$I_x = k_F W \frac{e\Delta_0}{2\pi\hbar} \frac{\sin(\Delta\varphi)}{\sqrt{(\cos^2(\Delta\varphi/2) + \zeta)(\zeta + 1)}} \tanh\left(\frac{\Delta_0}{2k_B T} \sqrt{\frac{\cos^2(\Delta\varphi/2) + \zeta}{\zeta + 1}}\right). \quad (5.10)$$

The high temperature critical current is

$$I_{c,\zeta} = \frac{k_F W e \Delta_0^2}{4\pi\hbar k_B T} \frac{1}{\zeta + 1} = \frac{I_{c,0}}{\zeta + 1}, \quad (5.11)$$

with  $I_{c,0}$  is the critical current without barriers (5.8). Figure 5.1 shows how the total current varies with the phase difference,  $\Delta\varphi$ , in the high temperature regime ( $k_B T = \Delta_0$ ) for different barrier strengths,  $\zeta$ .

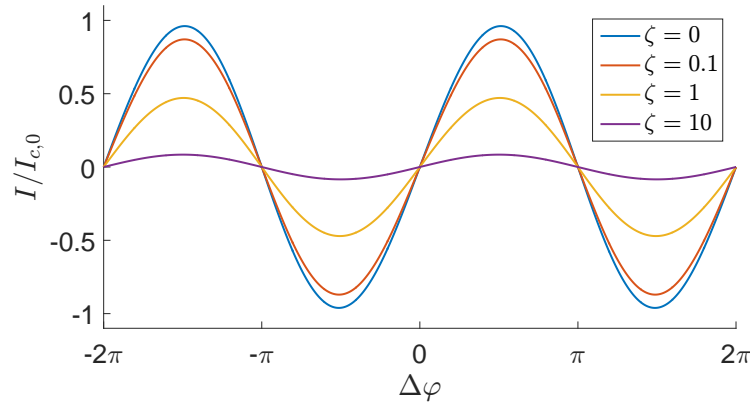


Figure 5.1: blabla

### 5.3 ABS current with applied field

With no barriers, but magnetic field we find the current from the ABS energy in equation (4.43):

$$\delta I_k(\Delta\varphi) = \frac{e\Delta_0}{\hbar} \sin\left(\frac{\Delta\varphi}{2} - \frac{\gamma_k}{2}\right) \tanh\left(\frac{\Delta_0 \cos\left(\frac{\Delta\varphi}{2} - \frac{\gamma_k}{2}\right)}{2k_B T}\right) \quad (5.12)$$

which in the high temperature regime ( $k_B T \gtrsim \Delta_0$ ), can be approximated to

$$\delta I_k(\Delta\varphi) \approx \frac{e\Delta_0^2}{4\hbar k_B T} \sin(\Delta\varphi - \gamma_k). \quad (5.13)$$

We notice that this expression is maximized when

$$\gamma_k = \frac{4n-3}{2}\pi + \Delta\varphi \quad (5.14)$$

with  $n$  as an integer. The Aharonov-Bohm phase shift,  $\gamma_k$ , will depend on the modulation and strength of the magnetic field, and on the trajectory of the particle. We will here consider three different modulations of the magnetic field. That is a uniform magnetic field (section 5.3.1), sinusoidal field varying along the junction (section 5.3.2) and sinusoidal field varying along the interfaces (section 5.3.3).

The magnetic field will be expelled in the superconducting region, due to the Meissner effect. We assume the penetration depth to be short even in the high-field regime, i.e. when  $l_m \lesssim L$  with  $l_m = \sqrt{\hbar/eB}$  as the magnetic length. The Lorentz effect will change the trajectories in the magnetic field into arcs of cyclotron radius  $l_{\text{cycl}} = \hbar k_F/eB = k_F l_m^2$ . However, we assume that  $k_F L$  is sufficiently large such that  $l_{\text{cycl}}/L = k_F L (l_m/L)^2 \gg 1$  for the fields considered and we can neglect the curvature of the trajectories.

#### 5.3.1 Uniform magnetic field

We will first consider a uniform magnetic field of strength  $B$ :

$$\mathbf{B} = B [\Theta(x + L/2) - \Theta(x - L/2)] \hat{z}, \quad (5.15)$$

and choose the gauge of the  $\mathbf{A}$ -field as

$$\mathbf{A} = -By[\Theta(x + L/2) - \Theta(x - L/2)]\hat{x}. \quad (5.16)$$

The Aharonov-Bohm phase shift,  $\gamma(x_0, y_0, \theta_k)$ , is calculated from equation (4.42) by integration along a path through the point  $(x_0, y_0)$  at an angle  $\theta_k$  with the  $x$ -axis, as shown in figure 3.1. The trajectory will be given by the line

$$y(x) = y_0 - x_0 \tan \theta_k + x \tan \theta_k. \quad (5.17)$$

Using this in equation (4.42) we find the phase shift:

$$\gamma = -\frac{2e}{\hbar} \int_L^R \mathbf{A} \cdot d\mathbf{l} = B \frac{2e}{\hbar} \int_{-L/2}^{L/2} y(x) dx = \frac{2L}{l_m^2} (y_0 - x_0 \tan \theta_k). \quad (5.18)$$

This expression is used in equation (5.12) and (5.3) in order to find the current density. The result from numerical computation is shown in figure 5.2 for three different magnetic lengths revealing the appearance of a row of current vortex-antivortex pairs. From equation (5.14) the current density is found to be maximum at  $x_0 = 0$  (at which the phase shift is  $\theta_k$ -independent) and

$$y_0 = \frac{l_m^2}{L} \left( \frac{4n-3}{4}\pi + \frac{\Delta\varphi}{2} \right). \quad (5.19)$$

Hence, the vortex lattice constant (the distance between two vortices) is

$$a_{\text{vortex}} = \pi \frac{l_m^2}{L}. \quad (5.20)$$

Figure 5.2 shows how the vortex lattice constant increases with the magnetic length. In the result we have taken the phase difference to be  $\Delta\varphi = \pi/2$ , however, the pattern looks identical for any  $\Delta\varphi$ .

In order to find the total current we combine equation (5.6), (5.3) and (5.12):

$$I_x = \frac{k_F}{2\pi} \frac{e\Delta_0}{\hbar} \int_{-W/2}^{W/2} dy_0 \int_{-\pi/2}^{\pi/2} d\theta_k \cos \theta_k \sin \left( \frac{\Delta\varphi}{2} - \frac{\gamma}{2} \right) \tanh \left( \frac{\Delta_0}{2k_B T} \cos \left( \frac{\Delta\varphi}{2} - \frac{\gamma}{2} \right) \right) \quad (5.21)$$

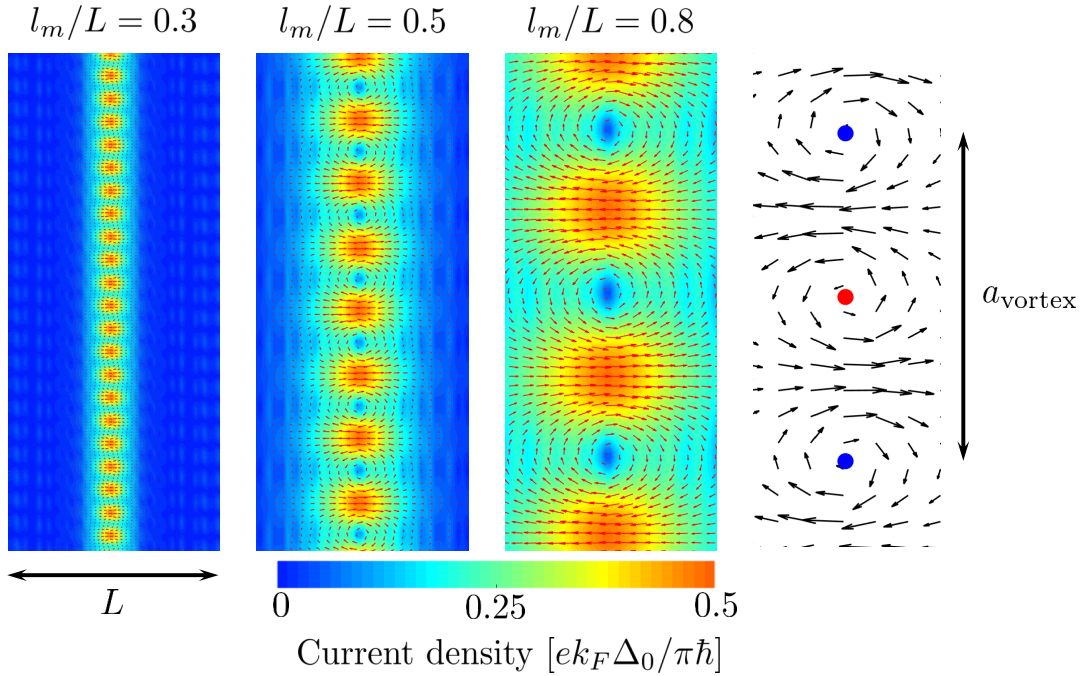


Figure 5.2: blabla

which in the high temperature regime ( $k_B T \gtrsim \Delta_0$ ) is simplified to

$$I_x = \frac{I_{c,0}}{2W} \int_{-W/2}^{W/2} dy_0 \int_{\pi/2}^{\pi/2} d\theta_k \cos \theta_k \sin(\Delta\varphi - \gamma). \quad (5.22)$$

From equation (5.18) we notice that  $\gamma(x_0, y_0, \theta_k) = -\gamma(x_0, -y_0, -\theta_k)$  which allows us to write

$$I_x = \frac{I_{c,0}}{W} \sin(\Delta\varphi) \int_{-W/2}^{W/2} dy_0 \int_0^{\pi/2} d\theta_k \cos \theta_k \cos \gamma. \quad (5.23)$$

The integral over  $y_0$  gives

$$\int_{-W/2}^{W/2} dy_0 \cos \gamma = \frac{l_m^2}{L} \sin\left(\frac{LW}{l_m^2}\right) \cos\left(\frac{2L}{l_m^2} x_0 \tan \theta_k\right) \approx \frac{l_m^2}{L} \sin\left(\frac{LW}{l_m^2}\right), \quad (5.24)$$

where the last equality is taken in the low field regime ( $l_m \gg L$ ) in order to simplify the analytical expression. The total current is thus

$$I_x = I_{c,0} \frac{\sin\left(\frac{e\Phi}{\hbar}\right)}{\frac{e\Phi}{\hbar}} \sin \Delta\varphi \quad (5.25)$$

with  $\Phi = BLW$  as the magnetic flux and we find the critical current at  $\Delta\varphi = \pi/2$ :

$$I_{c,\text{const}} = I_{c,0} \left| \frac{\sin\left(\frac{e}{\hbar}\Phi\right)}{\frac{e}{\hbar}\Phi} \right| \quad (5.26)$$

which is the well known Fraunhofer oscillations. The critical current resulting from numerical calculations is shown in figure 5.3.

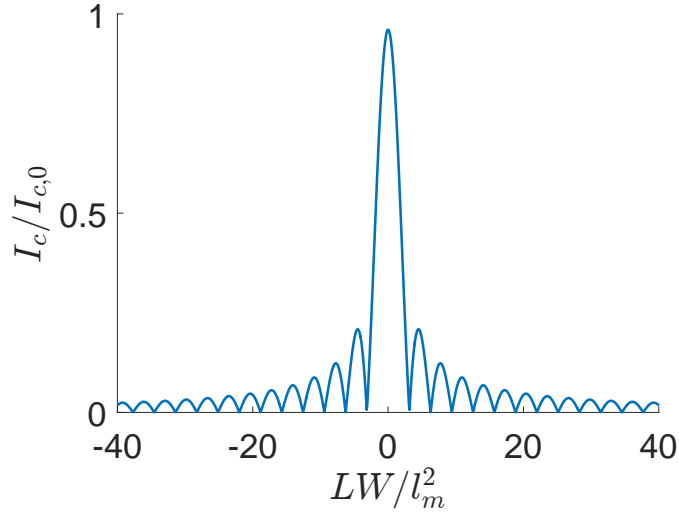


Figure 5.3: blabla

### 5.3.2 Sinusoidal field varying along the junction

We will next consider a sinusoidal magnetic field along the junction:

$$\mathbf{B} = B \sin\left(\frac{2\pi}{\lambda}x + \varphi\right) [\Theta(x + L/2) - \Theta(x - L/2)] \hat{z} \quad (5.27)$$

with the gauge

$$\mathbf{A} = -By \sin\left(\frac{2\pi}{\lambda}x + \varphi\right) [\Theta(x + L/2) - \Theta(x - L/2)] \hat{x}. \quad (5.28)$$

Again we use (4.42) and integrate along the trajectory in (5.17) to find the Aharonov-Bohm phase shift:

$$\begin{aligned}\gamma &= \frac{2}{l_m^2} \int_{-L/2}^{L/2} y(x) \sin\left(\frac{2\pi}{\lambda} + \varphi\right) dx \\ &= \frac{2\lambda}{\pi l_m^2} \left( [y_0 - x_0 \tan \theta_k] \sin\left(\frac{\pi L}{\lambda}\right) \sin \varphi + \frac{L}{2} \tan \theta_k \left[ \frac{\lambda}{\pi L} \sin\left(\frac{\pi L}{\lambda}\right) - \cos\left(\frac{\pi L}{\lambda}\right) \right] \cos \varphi \right).\end{aligned}\quad (5.29)$$

### Symmetric field

More specifically we let  $\varphi = \pi/2$  in (5.27) so that the magnetic field becomes symmetric about the  $y$ -axis and the second term in equation (5.29) is zero such that the phase shift is

$$\gamma = \frac{2\lambda}{\pi l_m^2} [y_0 - x_0 \tan \theta_k] \sin\left(\frac{\pi L}{\lambda}\right) = \gamma_{\text{uni}} \frac{\sin(\pi L/\lambda)}{\pi L/\lambda} \quad (5.30)$$

where  $\gamma_{\text{uni}}$  is the Aharonov-Bohm phase shift in the uniform magnetic field as given in equation (5.18). As this expression is proportional to the phase shift for uniform field we expect appearance of current vortices, but with a vortex lattice constant dependent on the wavelength of the magnetic field:

$$a_{\text{vortex}} = \pi \frac{l_m^2}{L} \frac{\pi L/\lambda}{\sin(\pi L/\lambda)}. \quad (5.31)$$

Hence, the distance between the vortices can be controlled not only by changing the magnetic field strength, but also by changing the wavelength of the symmetric field. For wavelengths  $\lambda = L/n$ , with  $n$  as a non-zero integer, we notice that  $a_{\text{vortex}} \rightarrow \infty$  and  $\gamma \rightarrow 0$ , such that we expect the vortices to vanish and the current to be unaffected by the magnetic field.

We can use  $\gamma$  (5.30) in equation (5.12) and (5.3) to calculate the current density numerically. The result is shown in figure 5.4 for three different wavelengths. We see how the distance between the vortices is changed when the wavelength of the magnetic field is changed, and that for some wavelengths, e.g.  $\lambda = L/2$ , the vortices vanish. The fact that the supercurrent survives for arbitrarily large field strengths,  $B$ , as long as the spatial modulation wavelengths satisfy  $\lambda = L/n$  is remarkable and is one of the key findings in this thesis.

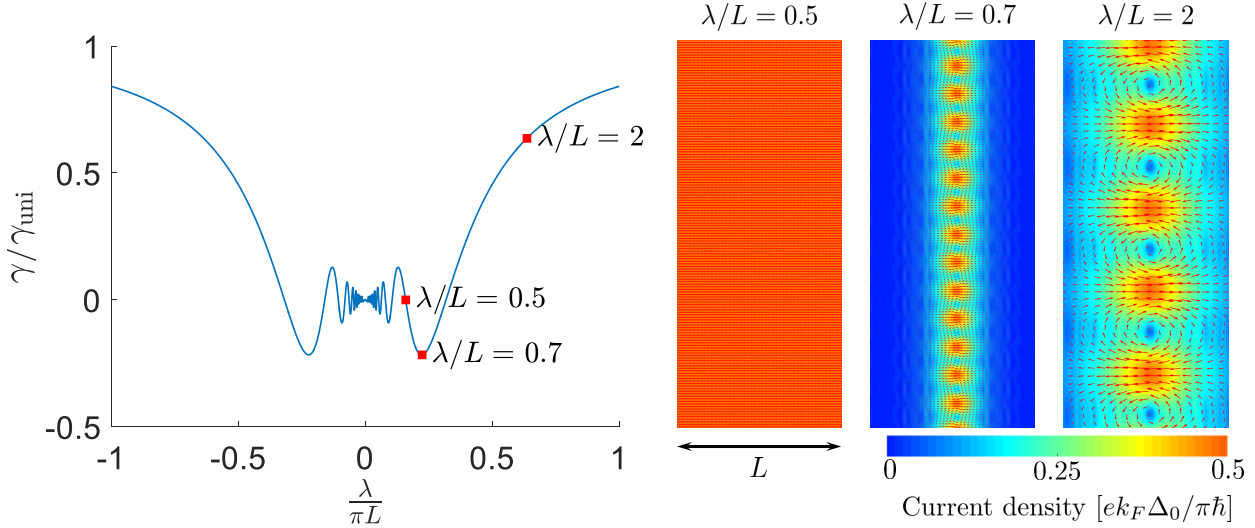


Figure 5.4: blabla

The total current is found in the same manner as in section 5.3.1, giving

$$I_x = I_{c,0} \sin \Delta \varphi \frac{\sin(\frac{e}{\hbar} \Phi)}{\frac{e}{\hbar} \Phi} \quad (5.32)$$

where  $\Phi$  is the magnetic flux:

$$\Phi = \int \mathbf{B} \cdot d\mathbf{A} = \Phi_{\text{uni}} \frac{\sin(\pi L/\lambda)}{\pi L/\lambda}, \quad (5.33)$$

with  $\Phi_{\text{uni}} = BWL$  as the magnetic flux in the uniform field. In terms of magnetic flux this expression is identical to the total current in the uniform field. However, the flux, and consequently the total and critical current, will be dependent on the wavelength. The high temperature critical current will be given as

$$I_c = I_{c,0} \left| \frac{\sin\left(\frac{LW}{l_m^2} \frac{\sin(\pi L/\lambda)}{\pi L/\lambda}\right)}{\frac{LW}{l_m^2} \frac{\sin(\pi L/\lambda)}{\pi L/\lambda}} \right|. \quad (5.34)$$

In figure 5.5 the critical current obtained from numerical computation is shown for different wavelengths,  $\lambda$ , and varying magnetic field strength,  $B$ . We recognize the Fraunhofer pattern as we had for the uniform field, but the decay can be controlled by changing the wavelength,  $\lambda$ , and for some wavelengths, e.g.  $\lambda = L/2$ , the critical current maintains constant regardless of the field strength. We propose that this can be understood as an interference phenomenon where

the phase-shift picked up by the electrons and holes comprising the ABS level are completely cancelled out due to the specific magnetic field profile.

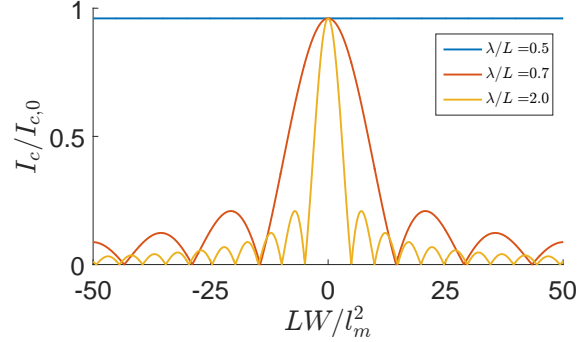


Figure 5.5: blabla

### Anti-symmetric field

Taking  $\varphi$  to zero in (5.27) the magnetic field becomes anti-symmetric about the  $y$ -axis, and the first term in (5.29) vanishes:

$$\gamma = \frac{L^2}{l_m^2} \tan \theta_k \left[ \left( \frac{\lambda}{\pi L} \right)^2 \sin \left( \frac{\pi L}{\lambda} \right) - \frac{\lambda}{\pi L} \cos \left( \frac{\pi L}{\lambda} \right) \right]. \quad (5.35)$$

We notice how  $\gamma$  now is position-independent and expect a uniform current distribution without current vortices. The magnetic wavelength dependency of  $\gamma$  is shown in figure 5.6(a). For certain wavelengths,  $\lambda$ ,  $\gamma$  will be zero regardless of the field strength or position and we expect the current to be unaffected by the magnetic field. Using the expression for  $\gamma$  (5.35) in equation (5.12) and (5.3) the current density is found numerically and the result is shown in figure 5.6(b) for varying wavelengths,  $\lambda$ , of the external field.

We find the total current in the high temperature regime as we did for the uniform field in section 5.3.1. As  $\gamma$  (5.29) is independent of  $y_0$ , equation (5.22) yields

$$I = \frac{I_{c,0}}{2} \int_{-\pi/2}^{\pi/2} d\theta_k \cos \theta_k \sin(\Delta\varphi - \gamma). \quad (5.36)$$

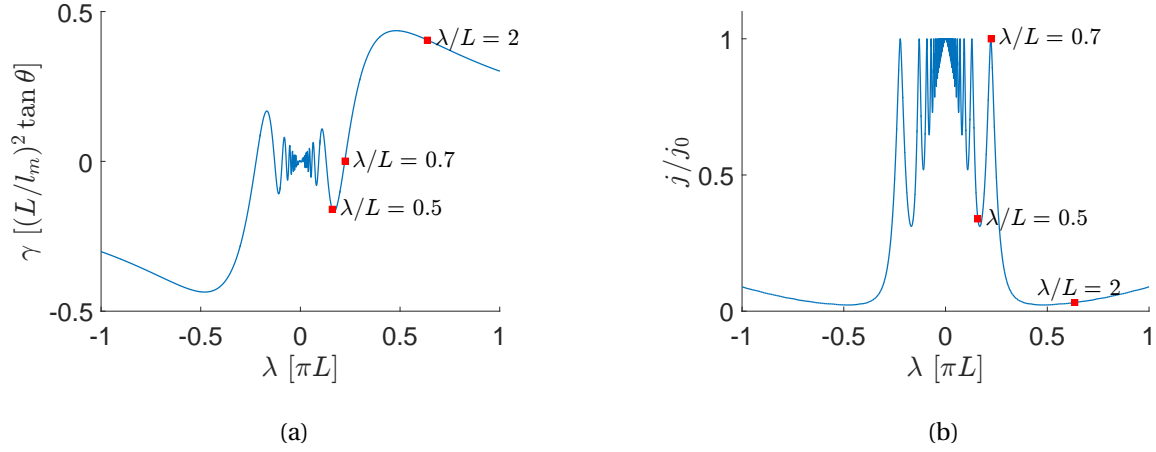


Figure 5.6: blabla

Using that  $\gamma(\theta_k) = -\gamma(-\theta_k)$  this can be rewritten to

$$I = I_{c,0} \sin \Delta \varphi \int_0^{\pi/2} d\theta_k \cos \theta_k \cos \gamma. \quad (5.37)$$

After inserting for  $\gamma$  and integrating over  $\theta_k$  we obtain the total current,

$$I = I_{c,0} \sin \Delta \varphi \frac{L^2}{l_m^2} |f(\lambda)| K_1 \left( \frac{L^2}{l_m^2} |f(\lambda)| \right), \quad (5.38)$$

where  $K_1(z)$  is the modified Bessel function of second kind and we have defined

$$f(\lambda) \equiv \left( \frac{\lambda}{\pi L} \right)^2 \sin \left( \frac{\pi L}{\lambda} \right) - \frac{\lambda}{\pi L} \cos \left( \frac{\pi L}{\lambda} \right). \quad (5.39)$$

Hence, the high temperature critical current is

$$I_c = I_{c,0} \frac{L^2}{l_m^2} |f(\lambda)| K_1 \left( \frac{L^2}{l_m^2} |f(\lambda)| \right). \quad (5.40)$$

The wavelengths  $\lambda$  that make  $f(\lambda)$  go to zero, will give  $I_c = I_{c,0}$ , regardless of the magnetic field strength. In figure ?? the critical current obtained from numerical computation is shown for different wavelengths,  $\lambda$ , and varying magnetic field strength,  $B$ . This result is in correspondance with the analytical expression (5.40). We notice that we no longer have the familiar Fraunhofer pattern and understand this as being a consequence of the absence of the current vortices. Just

like we found for the symmetric field there exists wavelengths, e.g.  $\lambda \approx 0.7L$ , which make the critical current  $I_c$  remain constant when the magnetic field strength increases.

### 5.3.3 Sinusoidal field varying along the interfaces

Instead of varying the field along the junction we will now consider a sinusoidal magnetic field varying along the interfaces:

$$\mathbf{B} = B \sin\left(\frac{2\pi}{\lambda} y + \varphi\right) [\Theta(x + L/2) - \Theta(x - L/2)] \hat{z} \quad (5.41)$$

with the gauge

$$\mathbf{A} = B \frac{\lambda}{2\pi} \cos\left(\frac{2\pi}{\lambda} y + \varphi\right) [\Theta(x + L/2) - \Theta(x - L/2)] \hat{x}. \quad (5.42)$$

Now the phase shift becomes

$$\gamma = -\frac{\lambda^2}{l_m^2 \pi^2 \tan \theta_k} \sin\left(\frac{\pi L}{\lambda} \tan \theta_k\right) \cos\left(\frac{2\pi}{\lambda} [y_0 - x_0 \tan \theta_k] + \varphi\right). \quad (5.43)$$

As we did in the previous section we will also here look at the symmetric- and anti-symmetric fields taking  $\varphi$  to  $\pi/2$  and 0, respectively.

#### Symmetric field

In the symmetric field, i.e. when  $\varphi = \pi/2$  the phase shift is

$$\begin{aligned} \gamma &= -\frac{\lambda^2}{l_m^2 \pi^2 \tan \theta_k} \sin\left(\frac{\pi L}{\lambda} \tan \theta_k\right) \sin\left(\frac{2\pi}{\lambda} [y_0 - x_0 \tan \theta_k]\right), \\ &= -\gamma_{\text{uni}} \frac{\sin\left(\frac{\pi L}{\lambda} \tan \theta_k\right)}{\frac{\pi L}{\lambda} \tan \theta_k} \frac{\sin\left(\frac{2\pi}{\lambda} [y_0 - x_0 \tan \theta_k]\right)}{\frac{2\pi}{\lambda} [y_0 - x_0 \tan \theta_k]}, \end{aligned} \quad (5.44)$$

where  $\gamma_{\text{uni}}$  is the phase shift in the uniform field. In the limit with  $\lambda \gg L$  and  $\lambda \gg y_0$  the phase shift will approach the phase shift in the uniform field,  $\gamma \rightarrow -\gamma_{\text{uni}}$ , as we would expect as a symmetric magnetic field will be approximately constant when the wavelength becomes very large. In the limit with  $\lambda \ll L$  the second factor in (5.44) will go to zero and the current density will be as if there was no magnetic field present.

In order to compare this field with the uniform field we consider the current density at  $x_0 = 0$  and  $\theta_k = 0$  in which the phase shift is

$$\gamma(x_0 = 0, y_0, \theta_k = 0) = -\gamma_{\text{uni}} \frac{\sin\left(\frac{2\pi}{\lambda} y_0\right)}{\frac{2\pi}{\lambda} y_0}. \quad (5.45)$$

Compared to the phase shift in the uniform field we have now an additional factor which will envelope the vortex rows we saw in the uniform field with a periodicity  $\lambda$ . The current density pattern will in this case depend on the phase difference  $\Delta\varphi$ , unlike what we have seen in the fields so far considered. We will consider two specific cases, namely  $\Delta\varphi = n\pi$  and  $\Delta\varphi = (n + 1/2)\pi$ , in which the the current density along the  $y$ -axis will be an even or odd function of  $\gamma$ , respectively, according to equation (5.13). When the current density is an odd function of  $\gamma$  we expect the vortex-antivortex rows for the uniform field to be repeated as rows and anti-rows of vortices with row lattice constant  $a_{\text{row,odd}} = \lambda$ . When the current density is an even function of  $\gamma$  we expect the vortex rows to be separated by a row lattice constant  $a_{\text{row,even}} = \lambda/2$ . Moreover, as the factor  $\sin(2\pi y_0/\lambda)/(2\pi y_0/\lambda)$  is an even function of  $y_0$  we expect the vortex rows to be symmetric about the  $x$ -axis, even when the current density is an odd function of  $\gamma$ . That is the pattern is such that if a row is placed at  $y_0$  then there is a corresponding row placed at  $-y_0$ .

The current density is found numerically from equation (5.12) and (5.3) and the result is shown in figure 5.7 for different wavelengths. We observe what was predicted, namely a repeated pattern of vortex-anti-vortex-rows. With  $\Delta\varphi = 0$  we observe rows and anti-rows separated by  $\lambda/2$  such that each row is separated by  $\lambda$ , i.e. row lattice constant  $a_{\text{row,odd}} = \lambda$ . With  $\Delta\varphi = \pi/2$  there are no anti-rows as the current density is an even function of  $\gamma$  and each row is separated by  $\lambda/2$ , i.e. row lattice constant  $a_{\text{row,even}} = \lambda/2$ . Moreover, the current density approaches a uniform distribution as  $\lambda \rightarrow 0$  with current as given in equation (5.7), as we predicted analytically. When  $\lambda \gg L$  the uniform field pattern reappears, as predicted. As the expression for  $\gamma$  is quite complicated we can not calculate the total current analytically, even in the high temperature regime. However, the critical current is found numerically and the result is shown in figure 5.8. For large wavelengths,  $\lambda$ , the critical current approaches the Fraunhofer pattern as we would

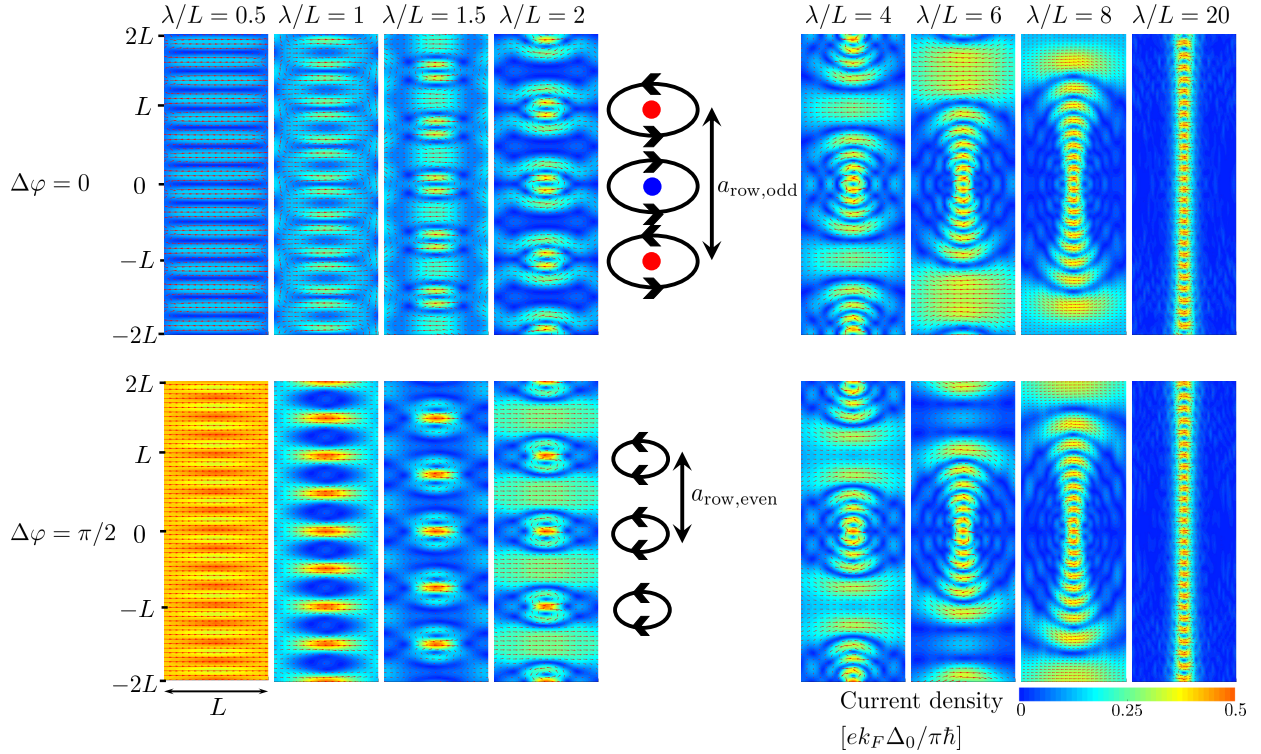


Figure 5.7: blabla.. Planen her å gjøre figurene litt finere sånn som for konstant felt. Og vise to rader med bilder, en med  $\Delta\varphi = 0$  og en med  $\Delta\varphi = \pi/2$

expect from the results found in the current density. Moreover, the critical current smoothens out and approaches the constant critical current  $I_{c,0}$  when the wavelength goes to zero.

### Anti-symmetric field

We now let  $\varphi = 0$  such that the magnetic field is anti-symmetric about the  $x$ -axis with the phase shift

$$\gamma = -\frac{L^2}{l_m^2} \frac{\lambda}{\pi L} \frac{\sin(\frac{\pi L}{\lambda} \tan \theta_k)}{\frac{\pi L}{\lambda} \tan \theta_k} \sin\left(\frac{2\pi}{\lambda} \left[\left(y_0 + \frac{\lambda}{4}\right) - x_0 \tan \theta_k\right]\right) \quad (5.46)$$

This is equal to the symmetric field (5.44), only shifted by  $\lambda/4$  along the  $y$ -axis. Hence we expect a similar, but shifted pattern as for the symmetric case. At  $\theta_k = 0$  and  $x_0 = 0$  the phase shift is

$$\gamma(x_0 = 0, y_0, \theta_k = 0) = -\gamma_{\text{uni}} \frac{\cos\left(\frac{2\pi}{\lambda} y_0\right)}{\frac{2\pi}{\lambda} y_0}. \quad (5.47)$$

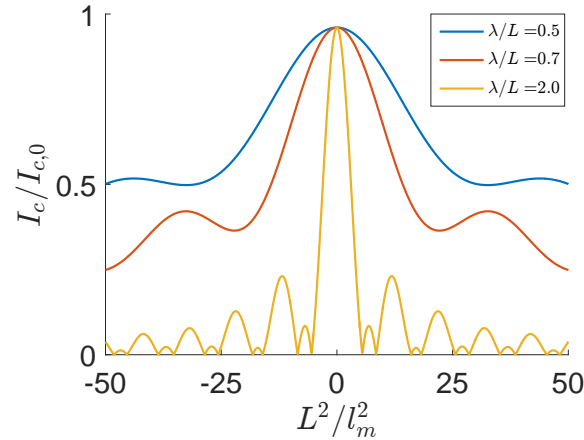


Figure 5.8: blabla

The factor  $\cos(2\pi y_0/\lambda)/(2\pi y_0/\lambda)$  is an odd function of  $y_0$  and unlike the symmetric case we now expect an anti-symmetric pattern about the  $x$ -axis if the current is an odd function of  $\gamma$ , i.e. when  $\Delta\varphi = n\pi$ . That is if there is a row placed at  $y_0$  there will be a anti-row placed at  $-y_0$ . This is confirmed numerically and the result is shown in figure (5.9).

Since the current density of the symmetric and anti-symmetric field along the interface only differ by a shift of the center of the vortex rows along the  $y$ -axis, we expect the total current to be equal in the two cases, when  $W \gg L$ . This has also been confirmed numerically, and the critical current will be as shown in figure 5.8.

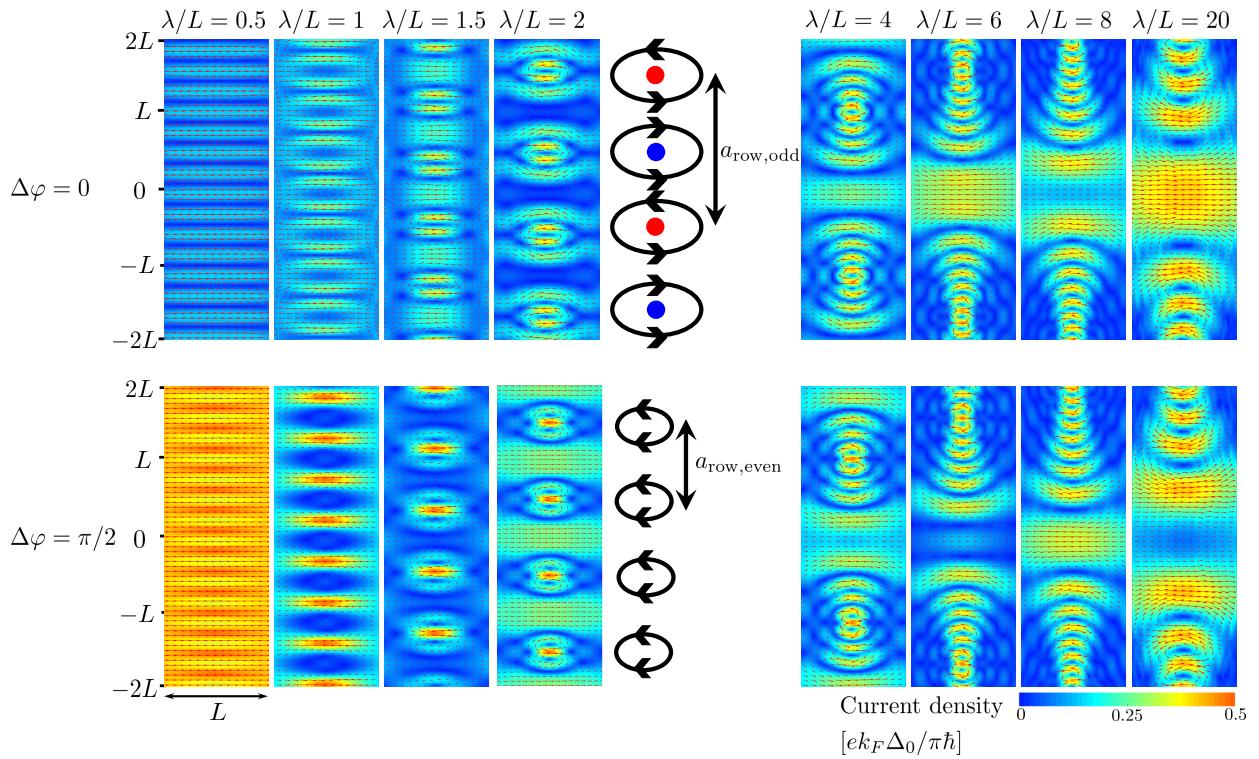


Figure 5.9: blabla.. Planen her å gjøre figurene litt finere sånn som for konstant felt. Og vise to rader med bilder, en med  $\Delta\varphi = 0$  og en med  $\Delta\varphi = \pi/2$

# Chapter 6

## Conclusion and outlook

In this thesis we have studied how the supercurrent density and the critical current in a SNS-junction is affected by an external magnetic field. The effect of a uniform magnetic field is already known !!!CITE!!!, however we have here considered modulated magnetic fields and seen how we are able to control the supercurrent via the magnetic field. One remarkable observation is that the supercurrent will be unaffected by the magnetic field for some modulations regardless of the field strength.

In chapter 4 we found the energy levels of the Andreev bound states which we in chapter 5 used to find the current density and critical current. We showed how the magnetic field accumulate a phase shift,  $\gamma$ , in the superconducting phase which depend on the field modulation and strength, as well as the trajectory of the electrons and holes, and thus give rise to quantum interference of the supercurrent. The modulations considered was a uniform field, a sinusoidal field varying along the junction and a sinusoidal field varying along the interfaces.

In the uniform field a row of Josephson vortices appeared in the center of the junction along the interface and the critical current was found to be the familiar Fraunhofer oscillations, in accordance with earlier research !!!CITE!!!. We found the same kind of vortex row in the symmetric sinusodial field varying along the junction. However, now the distance between the vortices could be controlled by changing the wavelength of the magnetic field and for some wavelengths we even found the current to be unaffected by the field. In the anti-symmetric field varying along

the junction the Josephson vortices and Fraunhofer oscillations disappeared leaving a uniform current density. The wavelength of the magnetic field could be used to control the magnitude of the current and for some wavelengths the current was unaffected by the field. In the field varying along the interface the vortex row that was observed in the uniform field was repeated as rows and anti-rows in the center of the junction along the interfaces. Unlike the uniform field, we then found the current density pattern to depend on the superconducting phase difference,  $\Delta\varphi$ .

In section 5.2 we found the supercurrent in a junction with barriers at the interfaces, but without external field. In future work it could be interesting to include barriers also in the external field. !!!CITE!!!. Moreover, we have here only considered a circular Fermi surface. In a uniform field with warped Fermi surface, earlier research has shown the appearance of a 2D-pattern of Josephson vortices, unlike the single row we have seen here. It could be interesting to also consider non-uniform modulations of the magnetic field for such Fermi surfaces. We have in this thesis ignored the spin-degeneracy of the electrons and holes. This degeneracy will give rise to the Zeeman-effect in the magnetic field !!!CITE!!!, and in future studies one could investigate the effect this has on the Josephson vortices and critical current.

# Appendix A

## Additional Information

### A.1 Commutation relations

$$[c_{\mathbf{k},\sigma}^\dagger, c_{\mathbf{k}',\sigma'}]_+ = \delta_{\mathbf{k},\mathbf{k}'} \delta_{\sigma,\sigma'} \quad (\text{A.1a})$$

$$[c_{\mathbf{k},\sigma}^\dagger, c_{\mathbf{k}',\sigma'}^\dagger]_+ = 0 \quad (\text{A.1b})$$

$$[c_{\mathbf{k},\sigma}, c_{\mathbf{k}',\sigma'}]_+ = 0 \quad (\text{A.1c})$$

### A.2 The pauli matrices

$$\sigma \quad (\text{A.2})$$

# Bibliography

- [1] W. Meissner and R. Ochsenfeld. Ein neuer effekt bei eintritt der supraleitfähigkeit. *Naturwissenschaften*, 21(44):787–788, 1933. ISSN 1432-1904. doi: 10.1007/BF01504252. URL <http://dx.doi.org/10.1007/BF01504252>.
- [2] A M Forrest. Meissner and ochsenfeld revisited. *European Journal of Physics*, 4(2):117, 1983. URL <http://stacks.iop.org/0143-0807/4/i=2/a=011>.
- [3] J. Bardeen, L. N. Cooper, and J. R. Schrieffer. Theory of superconductivity. *Phys. Rev.*, 108: 1175–1204, Dec 1957. doi: 10.1103/PhysRev.108.1175. URL <http://link.aps.org/doi/10.1103/PhysRev.108.1175>.
- [4] F. London and H. London. The electromagnetic equations of the supraconductor. *Proceedings of the Royal Society of London A: Mathematical, Physical and Engineering Sciences*, 149(866):71–88, 1935. ISSN 0080-4630. doi: 10.1098/rspa.1935.0048. URL <http://rspa.royalsocietypublishing.org/content/149/866/71>.
- [5] P. G. de Gennes. Boundary effects in superconductors. *Rev. Mod. Phys.*, 36:225–237, Jan 1964. doi: 10.1103/RevModPhys.36.225. URL <http://link.aps.org/doi/10.1103/RevModPhys.36.225>.
- [6] A. F. Andreev. The thermal conductivity of the intermediate state in superconductors. *Sov. Phys. JETP*, 19:1228 – 1231, Nov 1964. URL <http://www.jetp.ac.ru/cgi-bin/e/index/e/19/5/p1228?a=list>.
- [7] G. E. Blonder, M. Tinkham, and T. M. Klapwijk. Transition from metallic to tunneling regimes in superconducting microconstrictions: Excess current, charge imbalance, and supercur-

- rent conversion. *Phys. Rev. B*, 25:4515–4532, Apr 1982. doi: 10.1103/PhysRevB.25.4515. URL <http://link.aps.org/doi/10.1103/PhysRevB.25.4515>.
- [8] B. D. Josephson. Possible new effects in superconductive tunnelling. *Physics Letters*, 1(7): 251 – 253, 1962. ISSN 0031-9163. doi: [http://dx.doi.org/10.1016/0031-9163\(62\)91369-0](http://dx.doi.org/10.1016/0031-9163(62)91369-0). URL <http://www.sciencedirect.com/science/article/pii/0031916362913690>.